A STUDY OF DPPC AND DMPC MONOLAYERS AT DIFFERENT TEMPERATURES USING EPIFLUORESCENCE SURFACE BALANCE

AKRAM YOUSIF IBRAHIM

INFORMATION TO USERS

This manuscript has been reproduced from the microfilm master. UMI films the text directly from the original or copy submitted. Thus, some thesis and dissertation copies are in typewriter face, while others may be from any type of computer printer.

The quality of this reproduction is dependent upon the quality of the copy submitted. Broken or indistinct print, colored or poor quality illustrations and photographs, print bleedthrough, substandard margins, and improper alignment can adversely affect reproduction.

In the unlikely event that the author did not send UMI a complete manuscript and there are missing pages, these will be noted. Also, if unauthorized copyright material had to be removed, a note will indicate the deletion.

Oversize materials (e.g., maps, drawings, charts) are reproduced by sectioning the original, beginning at the upper left-hand corner and continuing from left to right in equal sections with small overlaps.

Photographs included in the original manuscript have been reproduced xerographically in this copy. Higher quality 6" x 9" black and white photographic prints are available for any photographs or illustrations appearing in this copy for an additional charge. Contact UMI directly to order.

Bell & Howell Information and Learning
300 North Zeeb Road, Ann Arbor, MI 48106-1346 USA
800-521-0600

A STUDY OF DPPC AND DMPC MONOLAYERS AT DIFFERENT TEMPERATURES USING EPIFLUORESCENCE SURFACE BALANCE

By

© Akram Yousif Ibrahim

A THESIS SUBMITTED TO THE SCHOOL OF GRADUATE STUDIES IN PARTIAL FULFILLMENT OF THE REQUIREMENTS FOR THE DEGREE OF MASTER OF SCIEMCE

DEPARTMENT OF PHYSICS AND PHYSICAL OCEANOGRAPHY

MEMORIAL UNIVERSITY OF NEWFOUNDLAND

CANADA

MARCH 2000

ST. JOHN'S NEWFOUNDLAND

Abstract

In this study some modifications have been introduced to the existing Epifluorescence Surface Balance (EFSB). Those modifications are essential for working at different temperatures. Phospholipid researchers are interested in revealing the mysterious behavior of certain phospholipids such as Dipalmitoylphosphatidylcholine (DPPC) which is the major component of lung surfactant. Many published studies have presented the surface pressure - area per molecule isotherms of DPPC and Dimyristoylphosphatidylcholine (DMPC) at different temperatures. In this study isotherms of DPPC and DMPC in the temperature range from 14 °C to 42 °C and from 6 °C to 23.3°C respectively, have been constructed after modifications have been introduced. A good agreement between the published isotherms and the ones presented here is obtained. The isotherm technique has been found invaluable, but may be usefully complemented by other techniques for obtaining information about the phase behavior of lipid monolayers at the air/water interface.

Unfortunately, there are not many published studies at higher temperatures in the field of visualization of the phospholipid monolayer domains. The problem of subphase condensation on the surface of the objective lens and other problems have prevented researchers from carrying out such studies. In this study the problem of the condensation has been minimized by introducing a technique of "Teflon Sleeve" heater. Some stimulating results are presented concerning the visualization of domains of DPPC at temperatures in the range from 18 °C to 35 °C.

The study presented in this thesis can be useful to researchers who are interested in visualizing the domains of DPPC and monitoring their behavior at temperatures near to physiological temperature, which is 37 °C.

The domains of DMPC also have been visualized at temperature of 5 °C. Unfortunately, the DMPC domains have not been recorded due to their small size. The limitation in the resolution of our recording system has prevented that recording.

Fundamental literature about phospholipid monolayers - particularly DPPC and DMPC- is presented in chapters one and two. The experimental set-up of the EFSB is discussed in chapter three. The results, which have been obtained in this study, are discussed in chapter four.

Acknowledgements

I like to take this opportunity to express my sincere gratitude to all individuals who supported this work. In particular I thank my supervisor Dr. Nathan H. Rich for the constant and valuable support, guidance, and stimulating discussion, Dr. Svetla Taneva and Ms. June Stewart-Department of Biochemistry MUN- for valuable assistance in chemical preparations and discussion. Also I acknowledge the help of Dr. M. Clouter, Dr. R. Goulding and Mr. C. Stevenson, in fixing computer and printing problems. I am thankful to Mr. Don Fillier, Mr. Carl Mulcahy from the Department of Technical Services, and Mr. Bill Kiely from the Department of Physics, MUN, for constructing parts of the Epifluorescence Surface Balance. I am also grateful to the Head, Graduate Studies coordinator and staff of the Department of Physics. I extend my thanks to the School of Graduate Studies at Memorial University of Newfoundland for financial support.

Table of Contents

List of Tables

List of Figures

CHAPTER ONE

GENERAL INTRODUCTION and OVERVIEW

1. General Introduction

Monolayers or monomolecular films are those films formed at the air/water interface, with one molecule in thickness. Some organic molecules when spread on the surface of water follow this special arrangement. The molecules tend to minimize their free energy. Those molecules consist of two parts, a polar head that loves the water (hydrophilic) and a hydrocarbon group or tail that hates the water (hydrophobic). Such a molecule is called *an amphiphile*. At the surface of the water the organic film will be with the head group in the water and the tail in the air.

A stable monolayer film is obtained when the forces due to adhesion between the *amphiphilic* molecules and the water are greater than the cohesion force between *amphiphiles* themselves [1].

1.1 Monolayer materials:

The amphiphilic materials are the materials forming monolayer films. Phospholipids and long-chain fatty acids are well known examples of these materials - Also they are called surfactants [1].

Phospholipid monolayers are popular in monolayer studies; they have been studied intensively. The driving force for the study on phospholipid monolayers originated from the important role they play in understanding biological cell membranes and their importance as models for the coating for the interior of the lung in air breathing animals. Among the most common phospholipid materials that have been studied by many scientists are Dipalmitoylphosphatidylcholine (DPPC),

Dimyristoylphosphatidylcholine (DMPC), and Dipalmitoylphosphatidylglycerol (DPPG). DPPC plays an important role in the lung surfactant; the monolayer formed by the artificial DPPC in vitro can be exploited as a model to simulate lung surfactant and cell membrane behavior in vivo. Detailed description for the monolayer applications is presented in section 2.14. In this work, light was shed on two of those phospholipids, DPPC and DMPC. Detailed presentation for the characteristics of DPPC is displayed in section 2.12.

1.2 Phases and Domains of Monolayer:

The most important phases of the monolayer under compression that can be shown by the π *vs.* A isotherm (section 1.4) are:

1.2.1 Gaseous: In this phase the molecules are far away from each other, and Van der Waals forces between them are very weak. The alkyl group (tail) will be laid at the surface of the water.

1.2.2 Condensed: With compression the packing and ordering of the molecules in the monolayer changes. In this phase the molecules are close and they have a limited freedom to move about. The alkyl chain will move a bit from the surface of the water, and the head group will be immersed inside the water.

W. D. Harkins has introduced the terms Liquid Expanded (LE) and Liquid Condensed (LC) phases [1].

1.2.3 Solid: This phase is attained by further compression. Molecules will be in closer contact with their alkyl groups straight up in the air -sometimes tilted- and their head groups in the water. Interactions between molecules are greater because of closer packing. Those phases are discussed in details in section 2.13 [1].

The domains of monolayer may be viewed when a suitable fluorescent dye is incorporated in the monolayer film. The molecules labeled with the dye stay in the expanded phase; these without dye group into the domains of the condensed phase. The shape of the domains is a result of competition between the force of the line tension that favors compact shape and the electrostatic repulsion that favors extended shape. The general consensus now -in phospholipid monolayer- is that the black domain is characterizing LC phase while the fluorescence from the incorporated dye is characterizing the LE phase.

1.3 Some useful definitions in monolayer studies:

The fundamental measurements in monolayer study are defined in terms of the following concepts.

1.3.1 Surface tension: γ: It is the force per unit length that tends to pull the molecules to the inner side of the liquid and thus minimize the surface area. That force is due to the unbalanced molecular attraction. It is identical to the surface energy per unit area. More detailed information about surface tension is presented in chapter two.

1.3.2 Surface pressure, π: It is the decrease in the surface tension of the water owing to the presence of the monolayer film. It is the most important parameter in the study of monolayers.

$$\pi = \gamma_{Water} - \gamma_{film}$$

1.3.3 Area per molecule: The area of the film divided by the number of molecules in it,

$$A = (A_t * M)/(C * N * V)$$

Where:

M is the molecular weight of the material.

N is Avogadro's Number.

V is the volume of the material.

C is the concentration of the material.

A_t is the area of the trough surface [1].

1.4 π *vs.* A isotherm:

This is a fundamental measurement in monolayer studies. With the monolayer under compression or expansion the changes in surface pressure (π) and area per molecule (A) are plotted in the ordinate and the abscissa respectively. The plot is constructed at a constant temperature. It provides useful information about the phase coexistence and transition of the monolayer films.

1.5 Properties of the monolayers:

They are one molecule thick, and when compressed they show different phases- two-dimensional analogies to gaseous, liquid, and solid phases in three dimensions. Their most important parameter is the surface pressure π, which the monolayer film exerts on the barrier.

1.6 Phospholipid Monomolecular Films' Temperature Dependence:

In the past the dependence of the behavior of such materials on temperature has been studied through the monolayer isotherm measurement. Many published studies have revealed the isotherms of phospholipids [2][3][4][5].

Scientists are hoping to elucidate the behavior of phospholipid monolayer at higher temperatures than room temperature. As an example, physicians are eager to reveal the characteristics of the DPPC at the physiological temperature -37 °C. Some researchers are interested in the critical phenomena that enable predicting the physical behavior of the monolayer material near its chain melting temperature.

To characterize the phase boundaries a powerful technique complementary to the isotherm technique can be utilized. This technique is known as Epifluorescence Microscopy. In this technique visualization of the domains has been achieved. There are not many published studies on the temperature dependence of the domains. Visualization of the domains at 25 °C has been reported [6].

1.7 Objective of This Work:

The importance of the role that is played by phospholipid monolayers in the lung surfactant and cell membrane provides the momentum that drives scientists to study the characteristics of such materials, especially at higher temperatures than room temperature. Some phospholipids and proteins were found to form a monolayer at the alveolar/air interface. That monolayer reduces the surface tension of the lung at expiration thus preventing the collapse of the lung during respiratory cycles.

Utilizing epifluorescence surface balance at higher degrees of temperature -such as 37 °C- is always accompanied by some thermal problems. Visualization observations at higher temperatures than room temperature require means to overcome experimental difficulties. At higher temperature, the subphase evaporates more rapidly and condenses on the surface of the microscope objective lens. The condensation on the lens prevents visualization of monolayer domains. That problem remains a prominent obstacle limiting the study of the domain formation at higher temperatures. Maintenance of uniform temperatures throughout the film requires careful technique.

The isotherms of phospholipid monolayer at different temperatures have been reported in many articles [2][7][8][9]. Unfortunately isotherms at higher temperatures do not provide sufficient information on phase behavior. The foregoing reason led researchers to concentrate their efforts on epifluorescence microscopy hoping that they can determine the behavior of monolayer phases at higher temperatures utilizing this technique.

In this work we have performed studies on DPPC and DMPC monolayers at different temperatures. We have been challenged by two experimental problems. The first

one is the thermal effect of the surface tension force measuring system -force transducer- when conducting experiments at higher temperatures. The force transducer is temperature sensitive, resulting in inaccurate surface pressure if uncorrected.

The second problem is owing to the condensation of the subphase on the objective lens at higher temperatures. We have developed a technique that has enabled us to eliminate the problem of the subphase condensation on the objective lens, by heating it and hence achieve visual observations of DPPC domains at higher temperatures. We report visualization at 35 °C and at the same time we have managed to eliminate the thermal effect on the force transducer and report isotherms of DPPC and DMPC at different temperatures.

The anticipated contribution of the technique reported in this study is that it can be utilized to achieve visual observations on domains of monolayer in general and in particular on phospholipid monolayers at the physiological temperature. The visualization of the domains of phospholipids at higher temperatures can yield valuable information that can help in elucidating the function and behavior of such material in lungs and cell membranes of living creatures.

CHAPTER TWO

THEORY

2. THEORY

2.1 Thermodynamical Variables of the Liquid Surfaces:

The study of the surface properties is very important for the workers in the field of monomolecular films because the fundamental characterizing quantities of the monolayers at the air/water interface are described in terms of those physical properties of the liquid surface. Some of those properties are discussed below.

2.1.1 Liquid –Air Interface:

The surface of a liquid is a very complicated thermodynamic system. It can be seen as a transition or boundary region between two different bulk phases of different composition and properties. In terms of molecular phenomena one can determine the most important properties of this region. One of these properties is the thickness of the interface. This thickness is very useful in determining the orientation of the molecules forming the films at the interface. The air/water interface is very important in the study of organic monomolecular films since it can simulate the environment of cell membrane and alveolar systems in living creatures [10].

I. Langumir has found that the thickness of the air/water interface is one or two molecules in thickness [11]. Some workers carried out studies of the interface region by the reflected light. From their measurements of the elliptical polarization of the reflected beam from the surface of the liquid, they have found that the thickness of this region confirms Langumir's findings [12][13].

Langumir in his paper [14] has explained the orientation of the large molecules at the interface. He introduced the principle of independent surface action. It states that in

molecules with ends 2-3 Å apart, the field of the force around each part will depend and be governed solely by the nature of that part, and will not be affected by the chemical nature of the other distant part. According to this principle, it was found that large molecules would arrange and orient themselves at the interface so that the polar head group will insert itself inside the water phase while the non-polar long chains will extend themselves at the air phase [10].

2.1.2 Surface Tension:

This phenomenon can be defined as the force due to unbalanced molecular attraction that pulls the molecules from the interface region to the interior part of the liquid and consequently leaves the interface with contracted small area [10]. See Fig. 2.1.

The surface tension determination represents a milestone in the studies of monolayer films spread at the air water interface [10].

Fig. 2.2 can be utilized to explain the surface tension. Atoms numbered 1,2,3, and 4 are representing the interface between liquid and gas phases. Atoms numbered 6,7,8,9,10 and 11 are representing the liquid bulk. Atoms numbered 12,13,14,15 and 16 are representing the bulk gas phase. r_o is the equilibrium interatomic separation. Atom numbered as 3 as an example, it must penetrate between atoms numbered 7 and 8 in order to proceed to the interior of the liquid. It must exert some energy $E_d^{\setminus}$. This energy is termed as activation energy for diffusion from the surface to the bulk. The atom needs such energy to separates atoms those are numbered 7 and 8, so that it can go between them. Also to overcome the weak force **f** due to attraction from gas atoms. The force **f** is very weak compared to that due to the attraction between atoms which are carrying the

numbers 3 and 8, for example. This is because the atoms in the gas phase are distant apart.

Now if we consider atom numbered 11, to overcome the attraction forces due to atoms numbered 9 and 10 besides to separate atoms numbered 7 and 8, it requires energy to fulfill those jobs in order to diffuse from the surface. The energy, which is needed for that is, termed the activation energy for diffusion from the bulk to the surface, E_d.

Obviously E_d' is less than E_d. This is because the magnitude of the forces to be overcome in the liquid bulk is greater than that of forces in the surface region. Because of that, it is easier for the atom to travel from the surface to the bulk than to travel in the reverse direction.

The magnitude of E_d' is continuously increasing with time, till diffusion rates from both phases are equal, at this point we reach a dynamical equilibrium, and E_d nearly equals E_d

If atoms numbered 3, 4, and 5 are taken as examples, the atom number 4 experiences attraction force $\mathbf{F(r_s)}$ due to atoms number 3 and 5. The surface consists of atoms with average intertomic distance r_s. Then the force per unit length of the surface, which is the surface tension, can be written as [15].

$$\gamma = F(r_s)/ r_s \qquad (2.1)$$

Adam in his book " The Physics and Chemistry of Surfaces" [16] has explained that the surface tension of the interface is merely the surface free energy needed to expand the surface. He explains that the surface tension is a hypothetical mathematical device usually used in the physics of surfaces, instead of the surface free energy.

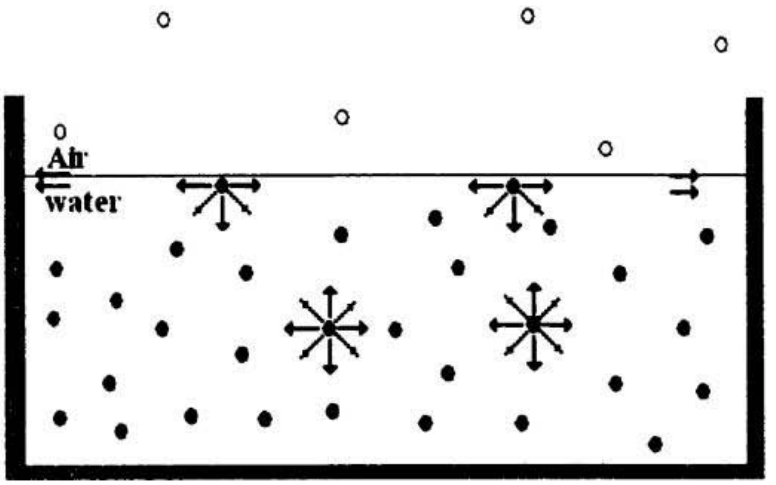

Fig. 2.1: The surface tension concept. Molecules at the surface experience an unbalanced force, while the ones inside the bulk are interacting with all the surrounding molecules. The air molecules are far apart. The arrows indicate the surface tension force.

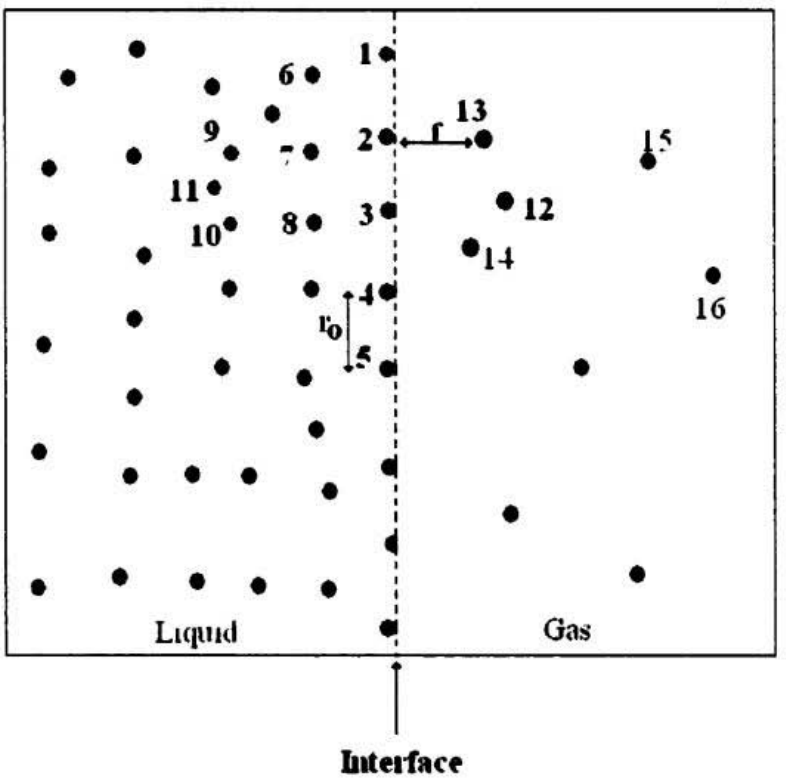

Fig. 2.2: Schematic illustration for explaining the surface tension. The dashed line is an interface between the air and water molecules.

This means that the surface tension force acting in parallel direction to the interface is itself the surface free energy per unit area [16]. See Fig. 2.1.

The surface tension has been exploited to calculate the surface pressure of the monomolecular film as will be discussed later.

2.2 The Dependence of Surface Tension on Temperature:

The relation between the surface tension force and the temperature can be explained using the atomic model. For a liquid in an equilibrium state with its vapor, as the temperature increases, the state of the liquid will move along the saturated liquid line (*ac*) in the phase diagram in Fig. 2.3.

Also the Vapor State will move along the vapor-saturated line (*ec)*. As the temperature increases, both of the states approach the critical point (C). At the critical point temperature, T_c, the two phases -vapor and liquid- are indistinguishable. The surface tension of the system will tend to zero. That is because the atoms that were at the interface and were governed by the attraction forces from the neighboring atoms in the liquid bulk, are now moving loosely and are indistinguishable from the atoms of the gas phase. This description reveals that there will be an interaction between atoms at the interface and gas atoms. Consequently, the unbalanced downward attraction that causes the surface tension will be compensated [15].

In general as the temperature of the liquid increases, the thermal energy of its molecules increases also.

The compensation of the unbalanced downward force that causes the surface tension can also explain why the solid film when placed at the interface can reduce the surface tension forces [15].

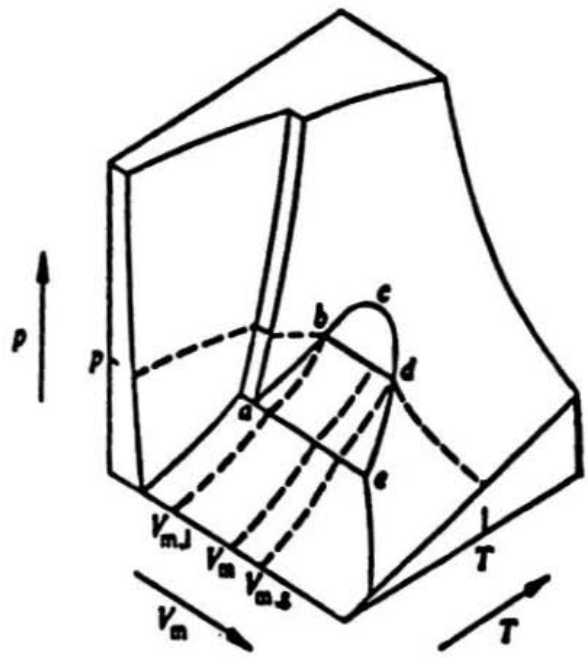

Fig. 2.3: Phase diagram for water. Redrawn from reference [15].

2.3 Monolayer Apparatus:

Some information from the literature about the development of the monolayer apparatus in general and its fundamental parts is presented here. The apparatus that has been utilized in this study is described in detail in the experimental set-up chapter - chapter 3. Figs.3.1 and 3.2.

The apparatus utilized by monolayer researchers is called Surface Balance. The surface balance has been used to spread monolayer, measure, and detect its properties. Nowadays, advanced surface balances with a lot of modifications have emerged. The fundamental concept is shared by all of those versions. The first idea of constructing surface balance has been introduced by Wilhelmy in 1863. In this version, the surface tension of a liquid was measured by dipping a plate in the liquid. At the same time similar measurement of the surface tension of clean water was carried out. Comparison between the two measurements has yielded what is known as the Surface Pressure (π)[10].

Dervichian, Anderson, and Harkins have carried out implementation and improvements to the Wilhelmy method [10]. They observed deflection of a scale with a spot of light reflected from a mirror. The deflection was due to the motion of the slide that indicates the net force on the plate. They have partially immersed the Wihelmy plate in a clean water surface. The plate was hung from one beam of a balance. Dubois and Mauer introduced more improvements. These were in forms of electrical actuation recording system and fixed plate positioning [10].

I. Langumir has presented his modifications to the Wilhelmy balance in his report in [11]. In this version he managed to overcome some of the drawbacks of Wilhelmy's, such as the problem of the angle of contact between the liquid and the dipping plate. This

problem has been found to affect the sensitivity of surface pressure measurement [17]. Full description of the Langumir surface balance can be found in his paper of 1917 [11].

All the modern versions of the surface balances are based on the same concept as Wilhelmy's and Langumir's.

2.4 The Monolayer subphase:

The subphase is a liquid that serves as a medium on the surface of which the monomolecular film is deposited. Frequently double distilled water is a suitable subphase. It should be very pure and clean from contaminants and surface-active impurities like Al^{+3}. A very small amount of Al^{+3} was found to cause a serious problem of contamination [18]. Some researchers have tested the effect of divalent cations, when dissolved in the double distilled water, on the separation of monolayer phases [19][20]. The subphase that has been used in this study is described in section 3.7.

2.5 Fundamental Parts of Surface Balance:

All the surface balances share the following fundamental parts:

2.5.1 Trough:

The workhorse of the insoluble monolayer investigations is the Langumir trough. It is a tray where the liquid subphase is put and the pressure-area isotherm is generated [2]. It should be of relatively large surface area so that a substantial compression can be achieved. In addition it must be accessible for manipulation and resist contamination. The trough material should be non-wettable; suitable materials satisfying this are hydrophobic [10]. Some researchers have tried materials like brass, gold, and aluminum

to construct the trough. They have been confronted by contamination problem [18]. Teflon material is the best choice for meeting all requirements. Zisman was the first one who has introduced it [21]. Some modifications were added to Zisman's trough and the outcome was the recent Teflon trough that is used nowadays [22][23].

2.5.2 The moving Barriers:

These are exploited to compress the monolayer film spread on the surface of the subphase. They are moving at the top part of the trough. They should be from a hydrophobic material. In addition they should fit well at the top of the trough so that the surface pressure will not push them up from the trough i.e. they should be relatively heavy. One of the disadvantages of the barrier method is the leakage at their edges.

Nowadays barriers are often replaced by a hydrophobic ribbon and thus the leakage is eliminated [10].

2.5.3 Flag [Wilhelmy Plate]:

It is a very thin piece of inert material. It could be glass, quartz, mica, platinum [10], or piece of filter paper [2]. Usually it is rectangular, with length l, thickness t, and width w. The equation used to calculate the force experience by this plate is based on the assumption that the thickness of the plate tends to zero ($t \rightarrow 0$), i.e. it should very thin. The plate serves as surface tension force sensor, meaning that it measures the force per unit area of the surface. [10]. The net force acting on the plate is:

$$F = \rho_p glwt + 2\gamma(t + w)\cos\theta - \rho_l gtwh \qquad (2.2)$$

which is the net of the gravitational force due to its weight, the surface tension that pulls

it downwards, and buoyant effect that acts upwards. ρ_p, ρ_l, γ are the densities of the plateand liquid materials and the surface tension force respectively. When the plate is completely wet, the angle of contact θ will be zero, ($\cos\theta = 1$). Then we can write the equation as:

$$\pi = -\Delta\gamma = -[\frac{\Delta F}{2(t+w)}] \tag{2.3}$$

where ΔF is the change in the net downwards force on the plate.

Assuming the force is constant, one can write:

$$-\Delta\gamma = -[\frac{\rho_l g t w}{2(t+w)}].\Delta h \tag{2.4}$$

Some workers have accounted for the effect of the water meniscus on the plate, and get more rigorous results [24][10]. In the recent surface balances the plate is hung from a rod that connects to a force sensor. It is partially immersed in the subphase. The sensed force on the plate will be coupled by a strain gauge force transducer and then recorded using an analogue to digital converter [7].

2.6 Phospholipid Monolayers:

The category of amphiphilic molecules includes a variety of types, such as phospholipids, fatty acids, certain proteins, biological membrane constituents, and other organic species [25]. These molecules when deposited on water surface will arrange their orientations spontaneously as has been described already in chapter 1. The formed arrangement will be one molecule in thickness. Thus one dimension is reduced to the thickness of one molecule; consequently we name these films as two-dimensional surface

films. Phospholipids are those lipids that contain a phosphate residue. The molecular formula for phosphatidylcholine is shown in Fig. 2.5.

Many features and characteristics are shared in phospholipid monolayers and other insoluble monolayers [10]. They are polar lipids that have stable and slightly soluble arrangement at the air-water interface. See Fig. 2.6 [26].

One importance of the phospholipid monolayers stems from the fact that they constitute half of the phospholipid bilayer. The phospholipid bilayer itself, with included proteins and other constitutes the building blocks of the living creatures' cell membranes.

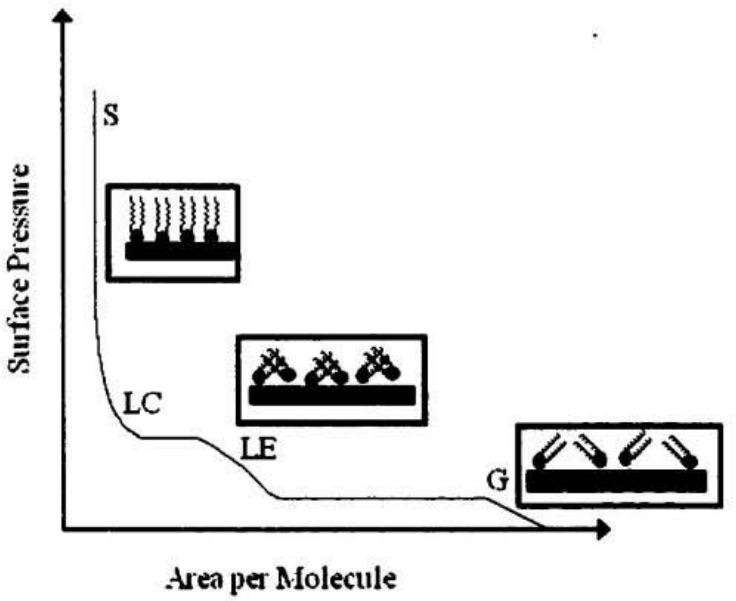

Fig. 2.4: Schematic illustration for the ideal surface pressure-area per molecule isotherm of phospholipid monolayer. Each state of the film has a certain characterizing order of molecules.

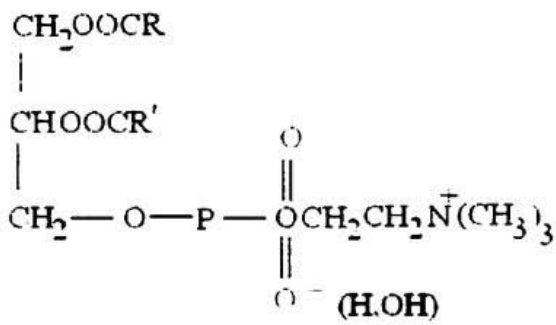

Fig. 2.5: The structure of the Phosphatidylcholine (Lecithin).

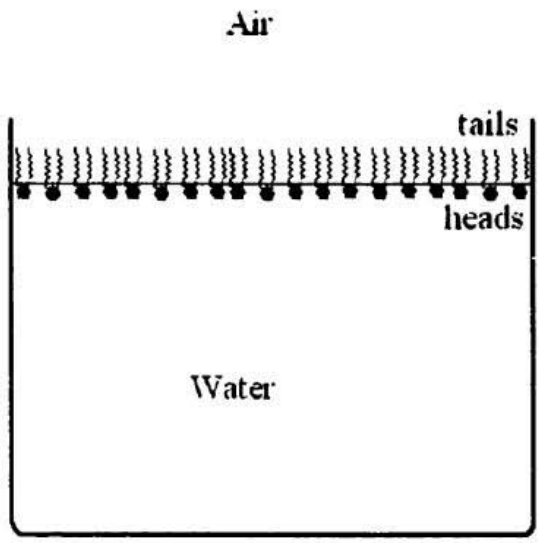

Fig. 2.6: The arrangement of the polar phospholipid molecules at the air-water interface.

2.7 Pulmonary Surfactant:

Pulmonary Surfactant is a film, thought to be a monolayer, which coats the lung alveoli to reduce surface tension decreasing the muscular force necessary to allow breathing [19].

The major components of the PS, in lipid fraction percentage, are phosphatidylcholine (PC) 74%, phosphatidylglycerol (PG) 10%, lysolecithin and sphingomyelin 5%, phosphatidylethanolamine 4%, and phosphatidylserine 2% [25][27]. Those lipids together with some proteins constitute a mixture of surface-active material at the alveolar-air interface [27][28]. During expiration the volume of the lung becomes minimal. The monolayer at this minimal volume will be compressed, and was found to reduce the surface tension of the alveolar fluid to zero [29]. The tensile properties in the alveolar fluid were found to enhance the lung compliance and thus the breathing process [29]. A team of researchers has found that the surface tension of the alveolar fluid at 37 °C - the temperature of the human body - is about one millinewton per meter [30]. S. Schürch and his co-workers have carried out experiments to relate the surface tension of the alveolar system at different temperatures. He has utilized an improved microdroplet method in order to achieve that [15].

In the medical field some reports have revealed that some prematurely born infants suffer the lack of the alveolar surfactant. This lack will result in the collapse of the lung during the breathing cycles [31]. This lack is called Respiratory Distress Syndrome (RDS). Another type of health problem occurs when some plasma proteins start to leak into alveolar fluid. This will result in disturbing the breathing process in older people. This is called Adult Respiratory Distress Syndrome (ARDS) [32][33][34].

Medical researchers and physicians have been searching for a suitable material to serve as a substitute for the natural surfactant. Ideally, this material would be produced artificially with the same properties as the real alveolar surfactant. They are hoping to infuse such material in the patients who suffer RDS or ARDS, so as to cure the malfunctioning of the lung [35]. The material should lower the surface tension of the alveolar fluid to zero when compressed to the lowest surface area. In addition it should have fast respreading and readsorption rates, and it should from a stable monolayer film at the alveolar-air interface [35]. Up to date it is not obvious to the researchers what is the exact composition of the surfactant mixture which will provide all the necessary conditions that allow the living lungs to function well.

B. Muller has reported that a mixture of proteins and lipids prepared artificially had been injected to some RDS and ARDS patients. The health conditions of those patients were improved [36]. Researchers are inspired by these research results and have started studying the components of the PS separately. Also they have tried to study their mixture under the same conditions of the living creature's lung. Continuing those experiments on the components of the lung surfactant, researchers are hoping to find a suitable artificial material that substitutes the real PS.

2.7.1 Dipalmitoylphosphatidylcholine (DPPC):

It is the major component of the PS mixture. Researchers during their search for a suitable artificial material to replace the lack of the PS have intensively studied the DPPC material. They have extracted it from animal lungs and deposited it in monomolecular films aiming to get useful and helpful information that can improve the understanding of its role in the breathing process [37][38][39][40].

It has been found that DPPC can easily be deposited on the surface of the water, and form a monomoelcular film. Also researchers have found that artificial DPPC material has the ability to decrease the surface tension of the water to zero millinewton per meter. Reduction of the surface tension force has been found when the monomolecular film is compressed to a minimal surface area. That is when the film is in a solid-like phase [41]. Since then DPPC has received great attention from monolayer workers. They have been thinking that DPPC is an important constituent of material that can serve as a PS substitute for patients of RDS or ARDS. Some workers found that the DPPC monolayer properties are not constant over a period of time [41]. π –A isotherms of DPPC have been reported in many articles [2][7][8][9]. Fig. 2.7 illustrates schematically the typical DPPC isotherm.

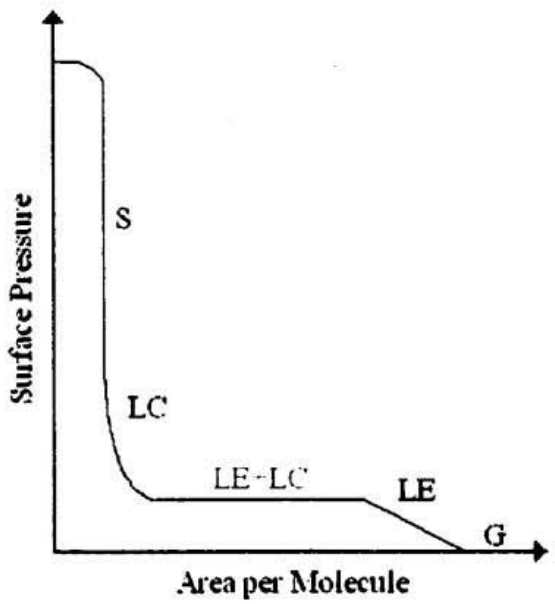

Fig. 2.7: Schematic illustration for the ideal surface pressure – area per molecule isotherm of DPPC. The physical states of the film are illustrated. In addition the plateau shows the coexistence of the two phases.

2.7.2 Dimyristoylphosphatidylcholine (DMPC):

DMPC displays similar features to other phospholipids. Many published studies have revealed the pressure – area per molecule isotherms of DMPC [42][43]. The stability of the monolayer of DMPC has been studied in a search for a suitable substitute for the lack of the PS components. J. Goerke has reported study on the collapse rate of the DMPC as a function of the temperature. He has concluded that DMPC would not be a good candidate for the mammalian surfactants. It has been reported that the melting chain temperature of DMPC is 24 °C [6][42]. The thermodynamical and phase transition parameters of DMPC have been presented in [43]. DMPC and DPPC have the same head group -phosphatidylcholine- but different hydrocarbon chain length. DMPC has chain length of 14 carbon groups while DPPC has 16 carbon groups in its chain. That difference influences their thermal behavior.

The bilayers of DMPC dispersion in water have been investigated. The permeability of water through the DMPC arrangement -bilayer- has been also revealed in [44][45][46]. The author of article [46] has suggested that at temperature of 29 °C, the evaporation of the water has been reduced by DMPC coverage. He has proven that the dispersion of the DMPC in water has an arrangement at the air-water interface that lowers the water evaporation rate. The author has found that all the properties and parameters of this arrangement are double that of a monolayer. He has concluded that the arrangement is merely DMPC bilayer [46]. The studies reported in [44][45][46] are revealing some puzzling information concerning the arrangement of DMPC at the air water interface. The authors have claimed that the arrangement is a bilayer instead of a monolayer.

Pure DMPC domain visualization is not reported in published literature, most likely because of the small size of those domains, beside the fact that the melting chain temperature of DMPC is about room temperature. The last fact results in the limitation of studying pure DMPC. The fluorescence microscopic visualization of the domains of mixtures of DMPC with cholesterol has been reported in [47].

2.8 Observation of Phospholipid Monolayers:

Two common techniques used to detect and visualize monolayer properties at air/water interface are (i) isotherm measurement and (ii) domain visualization under an appropriate microscopic system.

2.8.1 Isotherm measurement:

This provides one of the fundamental characteristics of the monolayer system. It reveals the two dimensional properties of the monolayer. K. J. Klopfer has described the kinks and plateaus as extremely valuable road maps that help in hunting down phase and ordering transition displayed by the monolayer film [2]. Old studies on monolayers of fatty acids have been performed utilizing the isotherm method. These studies have paved the way to many other studies on the phases of the monomolecular films [2][48].

As the monolayer is compressed at the air-water interface its surface tension decreases and the corresponding surface pressure increases. The surface pressure of the monolayer, as has been defined in section 1.3.2, is the difference between the surface tension of the pure water and the surface tension when the film is present. The general physical thermodynamic states -gas, liquid-expanded, liquid condensed and solid- of phospholipid monolayer can be observed in the isotherm. See Fig.2.4.

Many articles show DPPC and DMPC isotherms, below the melting chain temperature- which has been found by some workers near to 42.9°C and 24 °C respectively- [3][6][49], producing isotherms with lateral phase transitions and coexistence regions. One can see coexistence here -Figs.2.4 and 2.7- between the liquid condensed phase and the disordered liquid expanded phase [42][43]. A typical DPPC isotherm is illustrated in Fig. 2.7. At lower values for the area per molecules, point G, the molecules are far apart from each other. This represents the two dimensional gaseous state.

As the area per molecule is reduced by compression, the molecules start coming closer. This state can be described as a two dimensional liquid state. As more reduction of the area per molecule occurs, the molecules become closer than previous. This state is called the liquid condensed state (LC).

If more reduction of the surface area occurs, then the film will be in the two dimensional solid state (S). In this state molecules are strongly interacting with each other, and will be arranged in more ordered manner, with their tails up in the air above the surface. If more compression is applied after the appearance of the solid state the monolayer will collapse [50]. The collapse is detected when there is no increment in the surface pressure corresponding to decrement of the area per molecule. The collapse of DPPC monolayers has been found at high surface pressure at room temperature [41]. K. Nag has reported the collapse surface pressure for this material as 72 mN/m [25].

There is a region in the isotherm that shows a constant pressure line as the area per molecule changes. This plateau is an indicator for the region of coexistence between two phases. This region is associated with enthalpy changes [10]. O. Albrecht has

revealed that DPPC monolayer displays liquid expanded - liquid condensed coexistence region [10][37]. From the isotherm one can realize that there are changes of physical states of the film. The change of the state is due to packing and ordering of the molecules. This is termed as the phase transition. Researchers are hoping to improve their understanding of the features and details of the phase transitions of these films [42][51][52].

2.8.2 Seeing the Monolayer by Optical Arrangements:

The second method utilized to achieve monolayer detection is visualization.

For a long period of time, researchers have been looking for a device to enable them to visualize the morphology of a monolayer. The need of such technique stems from the fact that the isotherm method, some times, can not display all the important features of the monolayer when interesting physics is happening. To uncover the physics of the monolayer films, the need for additional technique has emerged. Researchers have tried microscopic techniques in order to achieve that. Electron Microscopy, Atomic Force Microscopy, and Brewster Angle Microscopy [53][54][55][56][57][58], are examples of the prominent traditional techniques that have been exploited to investigate the domain growth in the monolayer film. These techniques do not need any probe to be added to the film [2]. Some reports have revealed the utilization of Dark Field Electron Microscopy [59], and other methods are being developed e.g. Second Harmonic Generation and X-ray diffraction [60].

Some spectroscopic techniques have been also utilized to study the properties of the monolayer at the air/water interface such as Fourier Transform Infrared Spectroscopy

(FTIR), and Raman Scattering. These methods provide information about the positional order of the molecules in the film [61][62][63]. Direct visualization has been found to be a very useful complement to the other methods [2][64][65].

2.9 Domain formation:

Domains with their different morphologies are unique characterizing features for the monolayer. They mark the LE-LC phase transition, besides the two phase's coexistence region. The formation of the domains is a result of the competition between the line tension -that favoring compact circular shapes- and the electrostatic long-range repulsion between the dipole that favors extended shapes. The effect of impurities on domain formation has been studied. The impurities have been found to reduce the line tension and consequently that reduces the free energy for the creation of critical nucleus. One group of researchers has found that the relation between the impurity density and domain density is a linear one. The domain shapes of the phospholipid also have been reported to change to a curved shape and not to anneal for several hours [2][66][67].

The domain features such as shapes, sizes, and inter-domain distance, provide useful information concerning the equilibrium. The last feature was found to be a non-equilibrium property affected by impurity content in the film [68].

It has been found that domains with foam-like structure are formed in the Gas (G)/Liquid Condensed (LC) coexistence region. The domain dimensions were found to change with time. That suggests this is not an equilibrium structure [69][70][71]. In G/LC coexistence region, domains formed upon solvent evaporation. Their number increases upon compression. Their shapes were found to be constant with time. Due to the inter-

domain interaction, domain structure of phsophlipid monolayer was found to be deformed or distorted at higher domain density [66].

2.10 Fluorescence and Epifluorescence microscopies:

In 1981 Von Tscharner introduced a technique that has enabled monolayer investigators to see the monolayer film at the air-water interface. The technique is called fluorescence microscopy because it is based on seeing fluorescence from the monolayer.

It is a powerful and advanced technique that has revealed many intriguing monolayer properties. In addition it provides a means for direct observation of monolayer formation, phase, and phase transition. Besides that the technique has been suggested to be a suitable means for tracing the phase kinetics in two-dimensional systems [2]. The technique is based on observing the growth of shapes and sizes of the domains for a monomolecular film at the air/water interface. Domains are observed by incorporation of a fluorescent dye probe to the monolayer film [72]. The dye is incorporated in the monolayer solution at concentration of 1% to 2%. One can observe the fluorescence from the monolayer film when a suitable exciting beam irradiates it. Besides that the nucleating domains against the fluorescent background are also seen. The exciting light - which can be illuminated from the bottom or top of the trough - could be a laser or an arc lamp [2]. The lateral distribution of the dye can be determined through the analysis of the fluorescent image. The image of the fluorescent domain will be captured by a Charged Coupled Device (CCD) camera that is interfaced to a video monitor [2].

Those images are termed as micrographs. The micrographs are obtained due to the different dye solubility, fluorescence quantum yield, or molecular density of the

coexisting phases [69]. The dye has different solubility in the various monolayer phases. The fluorescent image reveals this lateral solubility separation of the dye. The dark domains are characteristic for the liquid condensed phase, while the fluorescent background is the liquid expanded phase [73][74].

Some researchers believe that since the dye probe is an impurity with different solubility in different monolayer phases the phase boundaries will be shifted by its presence. They have found that shift in the monolayer isotherm of the Pentadecanoic acid (PDA) is within the uncertainty of the isotherm measurement [2]. The isotherms have been found to be the same with and without the dye for sufficiently small dye concentrations.

The technique has become a popular one in the monolayer field. M. Lösche has reported visualization of phospholipid domains when he spread a phospholipid material at the air/water interface [75]. The technique has been found to be very useful especially for imaging the inter-domain textures and the domain shapes [76][77]. The shape and size of the domains of a certain monolayer are indications for the phases in that monolayer and their transition. A team of researchers has observed the nucleation of the domains against the fluorescent background [7]. They marked this to be the onset of the phase transition from liquid expanded to liquid condensed [76][77]. K. J. Klopfer has described phospholipid monolayers in different phases; the gas phase has been described as dark circular bubbles, L.E phase as the fluorescence from the background that will be seen as bright in the screen, and the LC phase as dark circular domains [2]. Others have agreed on those findings. In addition they have suggested that the condensed areas exhibit certain liquid crystalline properties [78].

The nature of the domain picture can be exploited to get useful information about the phase boundary and its thermodynamical variables [54]. Good agreement was found when the fluorescence results were compared with isotherm results for the Pentadecanoic acid (PDA) monolayer [54]. Despite the black and white nature of the fluorescence image, some researchers believe that the technique can be utilized to visualize more than two monolayer phases in equilibrium with each other. According to the authors of [2] this can be achieved by observing the evolution of features in the image.

The contrast between phases has been suggested to be due to the density variation and quenching of the dye in the gas region, but in the LE-LC coexistence region the contrast was found due to the smaller solubility of the dye molecules in the LC phase [79]. Some findings by researchers have revealed that the nucleating domains and their subsequent evolutions upon compression are independent of the dye concentration. They have proposed that the dye concentration should be very small in order to visualize clear phase boundaries. The same group of researchers has reported visualization of small brightly fluorescent spots -less than 2 μm in width- when they were studying PDA monolayer at 30°C. They have suggested they could be the crystallites of solid PDA, or it could be a signal of the dye precipitation inside the monolayer [79].

Monolayer workers have been disputing that LE-LC phase transition is a first order phase transition [79]. From the direct visualization of LE-LC coexistence domains some investigators have suggested that observation itself furnishes a convincing confirmation of the first order nature of that transition [79].

An epifluorescence microscope is a modified version of the traditional fluorescence microscope. In this technique the exciting light -which illuminates from

above the trough- and the fluorescence from the monolayer are both sent and received by the same objective lens. The domain picture is seen by a low light level video camera, and the images can be recorded on video tape that is interfaced to the system. The recorded images are later analyzed using menu-driven image software [80].

2.11 DPPC Domains:

The domains of dipalmitoylphosphatidylcholine -DPPC- have received much attention over the years. These were some of the first domains to be visualized by the fluorescence microscopy [69]. Researchers were aiming to exploit these domains to characterize the molecular orientational order at the air-water interface [81].

Many researchers have studied the shape and size of the domains of DPPC monolayers. Their shapes and sizes have been found to be dependent on the following variables: chirality of the molecule, temperature, the pH of the subphase, and externally applied electromagnetic field [80].

Quantitative study about domain sizes and their dependence on the compression rate has been carried out. The domains of the DPPC monolayer and their frequency distribution at two different speeds of compressions have been reported [80]. At fast speed of compression the domains were found to be irregular in shape, while at lower speed they were found to have different sizes with regular shape [80]. The author has illustrated the growth of the dark domains out of the fluorescent background. The dark domains have been reported to grow as finger-like projections occurring at the boundaries during compression. They also have been found to revert to more regular shapes during the period when compression was stopped. The domains have been found with kidney-

bean shape [80]. Some reports have investigated the visualization of "round" DPPC domains when compressing the monolayer very slowly. From those reports the authors have suggested that the stable shape of the DPPC domains is circular or bi-lobed [2].

Depending on the speed of compression, some authors have reported more than one shape for DPPC monolayer domains in the coexistence region. At slow compression -according to the literature between 0.2 and 8.0 $Å^2$/molecule.minute- the domains are nucleated as kidney bean-like shapes [2][80]. Their growth progresses from bean-like to S-like shape and then comes to the multilobe shape [2]. Other authors believe that the S-like and the multilobed shapes are simply fused combination of bean [81]. K. J. Klopfer has pointed out in his article about DPPC domains, that there can be significant amounts of different domain types in the co-existence region [2]. At a very fast speed of compression it has been suggested that the domains will have dendritic shapes [67][71].

Some authors have suggested that the kidney bean-like and S-like shapes in DPPC domains represent quasi-equilibrium morphology. They have deduced this result when they have seen those shapes upon compressing the monolayer very slowly [80][81]. K. J. Klopfer disagrees with those views. In addition he has suggested that circular domains are the equilibrium shapes for DPPC. He has allowed DPPC film to age overnight and then found circular domains had formed [2].

The effect of the rate of cooling on DPPC film has been studied. It has been found that the faster the cooling rate – cooling for half an hour- the higher the domain density, the shapes are S-like and bilobed. For lower rate of cooling-four hours- the kidney bean shape is the only shape that persists to lower density. These findings prove that the domain formation is a kinetically controlled process [2].

The fluorescence images of DPPC monolayer have been utilized to measure the fraction of the liquid condensed phase. This is by exploiting the lever rule [2].

2.12 Dependence of phase transition on temperature:

For a monomolecular film at the air-water interface, the physical states have been shown to be temperature dependent at fixed pressure. Some reports have revealed that the monolayer is very sensitive to temperature changes [43]. Utilizing the π-A isotherm, some investigators have shown that the surface pressure corresponding to LE→LC phase transition increases as the temperature increases [4][5][43]. M. C. Petty in his book - *Langmuir-Blodgett Films. An Introduction* - has reported LE→LC transition in two-dimensional monolayer is temperature and chain length dependent. The temperature increment has been correlated to the chain length decrement [1].

As mentioned previously, in a two-dimensional monolayer system, the driving force for the phase transition is the interaction between the molecules, namely Coulombic and multipole-multipole. If the temperature increases then the thermal motion of the molecules in the film will increase. This will result in leaving the film with expanded area, thus hindering LE→LC phase transition. It has been found that the reduction of hydrocarbon chain length by one methylene group-in case of long chain fatty acids- is equivalent to increment of the temperature by 5-10 K [1]. Decreasing the temperature has the reverse effect of course; i.e. it will decrease the thermal motion of the molecules, tending to condense the monolayer film. For DPPC isotherm, below a certain critical temperature -which was found to be 41 °C- one could observe the LE/LC coexistence region [4][5][43].

When changing the temperature, one can visualize the domain texture in the LE/LC coexistence region utilizing the fluorescence microscopy technique. Till now there are not many quantitative analyses on domain sizes and shapes as dependent on the temperature. Generally one can realize that the domains behave as LE domains as temperature increases. When approaching the kink of the LE→LC phase transition, then the domains of the LC together with the LE domains can be seen.

2.13 The Latent Heat of Transition:

In first order phase transitions, heat absorption or evolution always accompanies the changes from one phase to another at constant temperature. This heat is called the latent heat of transformation [1].

For monomolecular films one can determine the latent heat of the phase transformation by using the following equation:

$$Q_{main} = \Delta A(\frac{d\pi_c}{dT})T \qquad (2.5)$$

Where:

ΔA is the difference between the area where the film is totally condensed and the area where it is totally expanded. The areas are determined from the isotherm of the monolayer.

$d\pi_c/dT$ is the slope of plot of π_c - surface pressure at the onset of the coexistence region - *versus* the temperature. T is the temperature in Kelvin [3].

2.14 Applications of the monolayers:

The interest in studying the monomolecular films has been inspired in the recent decades. The driving force for this inspiration was the important role played by the monolayer arrangement in the fields of research and industry. The study of the monolayer has been found to provide useful information in many fields such as biological, chemical, pharmaceutical [82], medical, agricultural, and food science applications.

In industry the monomolecular films have been exploited in emulsions and foams, dispersion and enhanced oil recovery.

In the biological field, the monolayer arrangement has been used to investigate the phase transition in lipids. Moreover it was utilized to investigate the formation of vesicles, liposmes, bilayer and membranes [83].

The monolayer in general provides two important characteristics:

1- The single molecule nature that enables determination of the properties of the substance forming the monolayer.

2- The oriented nature of the monolayer molecules that facilitates the understanding of a tremendous number of natural phenomena. This provides a powerful technique to study the behavior of oriented molecules [10].

In the field of foam industry, the gas diffusion is an important process, the monolayer has been utilized as a model to study the transport of gas molecules [10].

The monolayer -being half of the bilayer- resemblance to the living cell membranes provides a good model to life science workers in order to study the membranes of the living cell, its properties and functions. Permeability, propagation, and

transportation of the nerve impulses mechanism can be understood exploiting the monolayer [84][85].

There is no doubt that the monolayer studies provide a good method for studying lipid-protein interactions in lung surfactant [80][86].

Technological applications for monolayers transferred from liquid to solid surfaces- known as Blodgett films- have emerged in the field of electronics [73]. Some investigators have reported utilization of monolayers in the fields of lubrication, ore floatation, and prevention of corrosion. In addition monolayer can be used as an analytical technique for the small amount of material forming the monolayer. This technique has been used to study adsorption of certain compounds from solution [87].

Monolayers have been exploited for evaporation retardant. This application is very important, especially in the area where water is in short supply [88][89]. An interesting application of Boldgett films is in the field of non-reflective multilayer coating for glass [90].

In physics studies the monolayer serves as a good model to investigate the two-dimensional systems [73].

CHAPTER THREE

EXPERIMENTAL SET-UP, MODIFICATIONS, AND MATERIAL PREPARATION

3. EXPERIMENTAL SET-UP, MODIFICATIONS, AND MATERIAL PREPARATION

Based on Wilhelmy method, Kaushik Nag - with help of Dr. K. Keough, Dr. N. Rich, C. Boland, and others- has built the surface balance that has been utilized in this study [7]. The major components of the balance are illustrated in Fig. 3.1. Some modifications in the compressing and controlling systems have been introduced in order to prevent the leakage of the film at higher surface pressure.

The parts of the balance can be categorized in the following systems:

1- Spreading and compressing systems.

2- Force measuring system.

3- Microscopic components.

4- Recording and controlling system.

5- Additional accessories.

3.1 Spreading and compressing systems:

This part of the set-up consists of a trough and a closed ribbon. Dr. N. Rich has designed the trough and the construction has been performed at Memorial University of Newfoundland Technical Services workshop. The material of construction is Teflon. The trough has a cavity of the following dimensions: 22 x 7.8 x 1.5 cm. The dimension choice is based on the accuracy of the measurement for the area per molecule. The compressing system has been changed from the barrier method to the ribbon method to avoid the leakage problem at high surface pressures. To change the temperature of the subphase in the trough, an aluminum base is fixed to the bottom of the trough. Hot or cold water can be circulated via channels inside the aluminum base. The circulation of the water with a

selected temperature for a sufficient period of time will yield a desired temperature at the subphase.

Inside one end of the cavity of the trough, a twin-well piece with dimensions 15x 6.4 x 1.9 cm. -made of Teflon- has been located. The diameters of the two wells are 3.11± 0.1 cm and 3.16 ± 0.1 cm. respectively. This piece was intended to decrease the motion of the subphase, and hence improve the quality of the fluorescent images. See Fig. 3.4. The trough is put in XYZ translator in order to facilitate and control the positioning of the trough. Focusing is accomplished with a piezoelectric micrometer for vertical motion.

The compression process for the monolayer film at the surface of the subphase can be achieved by utilizing a closed ribbon. The ribbon method compared to the moving barrier one was found to eliminate the film leakage problem. Four small Teflon pegs - of 0.6 cm. in diameter - stretch the ribbon. Each pair of pegs is fixed to an aluminum bar. One of the bars slides along the top part of the trough frame. A bi-directional linear actuator stepper motor (Airpax, L92411-p1, Cheshire, CT) that pushes a twelve inch threaded shaft achieves the movement of the rod. The shaft is connected to the moving bar. By this means, the area enclosed by the ribbon can be decreased or increased corresponding to compression or expansion respectively. The motion of the bar comes to a complete stop when it hits one of the two roller-type limit switches installed at the ends of the trough. The actuator motor is controlled by a stepper motor controller board (Metra Byte, MSTEP-5 Tannton, MA) with accessory board (Metra Byte, STA-STEP). This combination provides a wide range of motor speed. The IBM-AT compatible personal computer has been interfaced in order to control the motor motion.

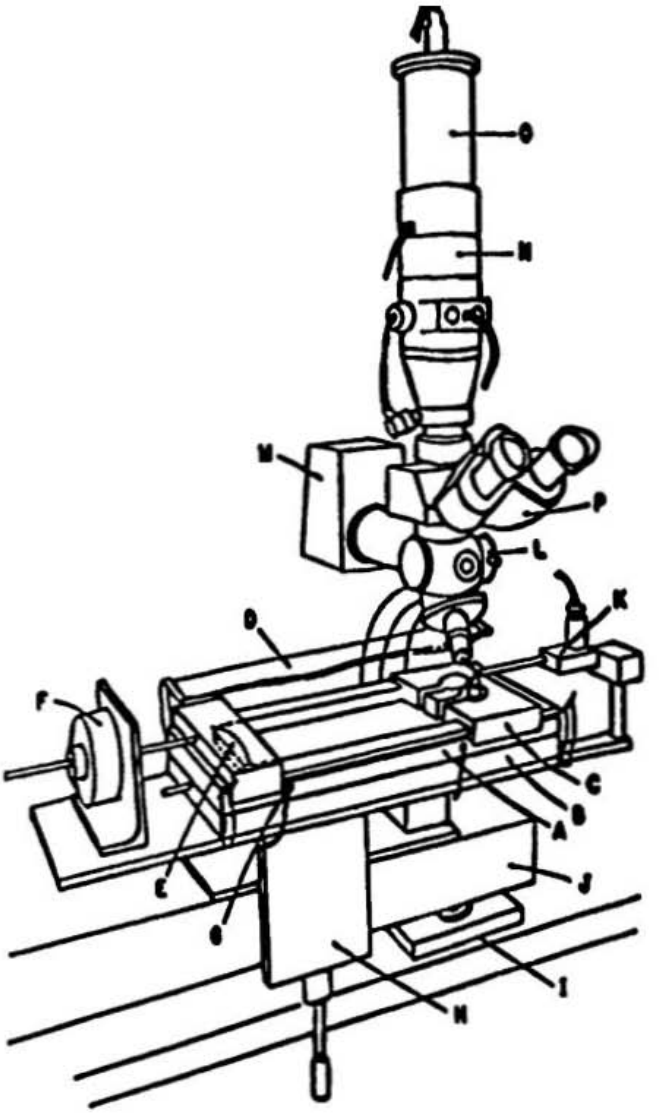

Fig. 3.1: Illustration for the components of the Epifluorescence Surface Balance-Redrawn from reference [7].

Teflon Trough (A), Aluminum Base (B), Teflon Collar (C), Plastic Cover (D), Movable Teflon Barrier (E), Stepper Motor (F), Limit Switch (G), X-Y-Z Translator (H), Vibration Isolation Support (I), Granite Base (J), Force Transducer (K), Fluorescence Condenser (L), Light Source (M), Image Intensifier (N), CCD Camera (O), and Trinocular Tube (P).

3.2 Force measuring system:

A Wilhelmy plate senses the surface tension force of the subphase in the trough. The plate is made of platinum with dimensions 2.5 x 1 x 0.25 cm. The plate is hung from a rod that is connected to a force transducer (Grass, 5f58, PO, Quincy, MA). The sensitivity of the force transducer is 20 mm/kg. The net force on the plate can be read by a strain gauge DC amplifier connected to the force transducer. The strain gauge transfers the data through an A/D converter (Metra Byte, Das-8). The data then is forwarded to the computer system by the acquisition system. Computer software TEMP6 - written in C-language - combines the signal from the transducer and motor step information, and then displays the surface pressure versus area per molecule graph, i.e. π-A isotherm. See the block diagram in Fig. 3.3.

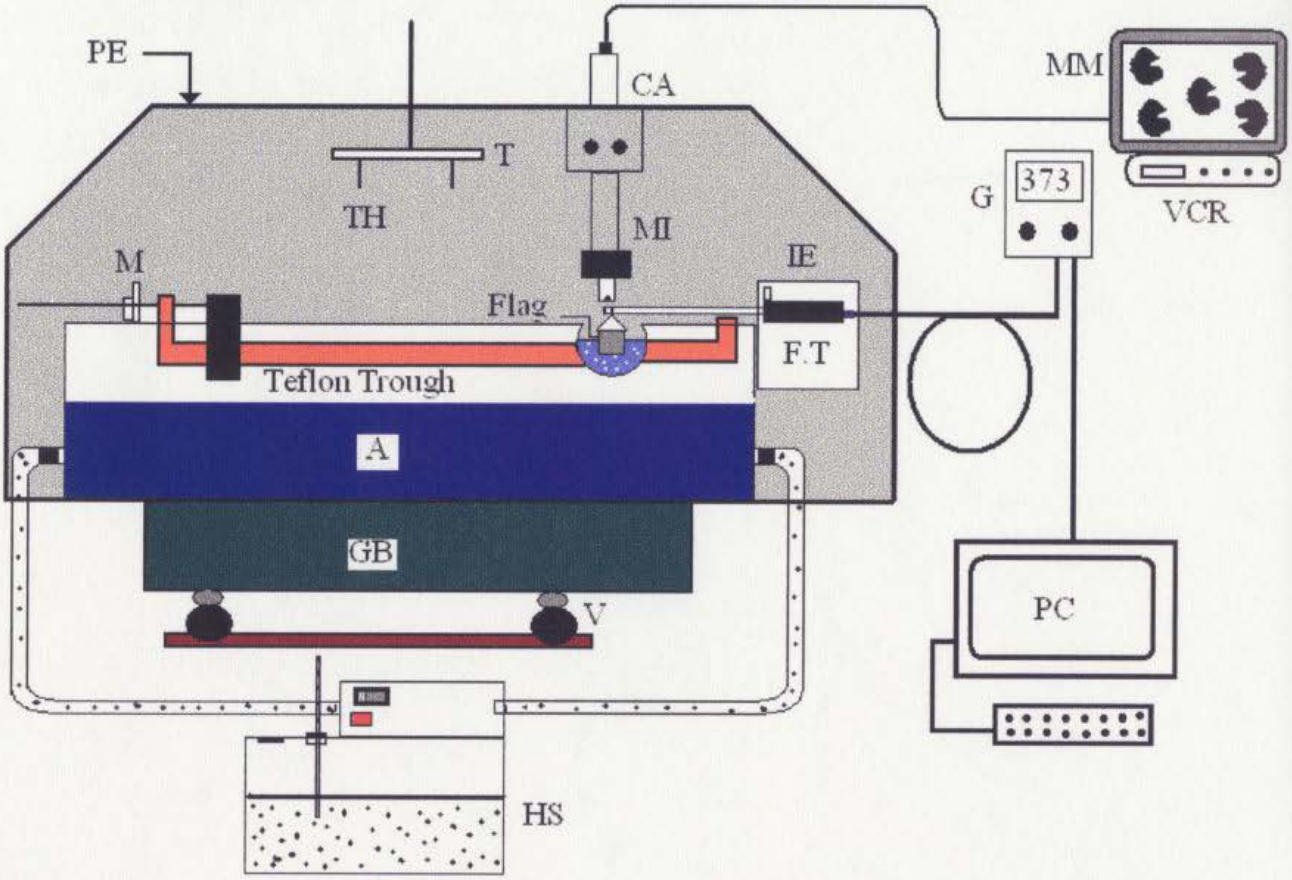

Fig. 3.2: Schematic illustration for a cross section view of the Epifluorescence Surface Balance. The plastic cover (PE), the low level camera (CA), the monochromatic monitor (MM), the video (VCR), the stepper motor (M), the thermocouples (TH), the supporting Teflon plate (T), the microscopic system (MI), the strain gauge amplifier (G), the force transducer (FT), the aluminum base (A), the granite supporting base (GB), the vibration damping system (V), the personal computer (PC), the heating/cooling pumping system (HS), and the isolating enclosure (IE).

3.3 Microscope components:

The balance has been equipped with a microscope. The arrangement enables the observation of fluorescence from the monolayer. The fluorescence can be generated as a result of exciting the molecules of the dye by a suitable light source. The source should have emission wavelength corresponding to the absorption band of the dye molecules. The suitable exciting light for our experiment is sent from a 50 W mercury-vapor lamp. (Zeiss HBO 50 W). An epifluorescence condenser (Zeiss Type IVF1) was added to the microscopic system recently. The objective is utilized to send the exciting light and at the same time to receive the fluorescence from the monolayer. A set of epifluorescence filters (Zeiss, type ES16) - that permits observing the wavelength of the fluorescencent beam from the dye molecules- is exploited. The filters have band pass 485/20, excitation FT510, wide emission LP520 filters that enable seeing the green fluorescence [80]. Other probes can be utilized in this set-up. Those probes have characteristic absorption/emission wavelengths requiring individual filter sets. This allows for example, monitoring separately tail and head groups, or proteins incorporated in the film [91].

The fluorescence from the dye is captured by a detecting system. The detecting system that provides the image consists of objective lens, a camera, and a monitor.

The objective used for most of this work has magnification 40X (another of 50X was used as well). It has very short working distance. The magnification -which is provided by a combination of the objective, trinocular tube, camera, and monitor- is about 5000 times. The high resolution of the system enables detecting any structural shape in individual domains.

3.4 Recording and controlling systems:

The epifluorescence surface balance is interfaced to IBM-AT compatible personal computer. The controlling code - which has been written by Mr. Carl Boland - Memorial University of Newfoundland - is installed in this computer. The code has the ability to calculate the surface pressure, area per molecule, surface tension, and the percent of the pool area. Also it displays the monolayer isotherm beside the graph of the percent area of the pool versus the surface tension. The plots can be stored in a file to be recalled later.

Concerning the domain images, utilizing a low light level video camera (Fairchild Corp, CCD3000, Palo Alto, CA) in tandem with image intensifier (Varo, 25 mm MCP, Garland TX) one can observe fluorescent intensities from the monolayer.

Charged Couple Device (CCD) chip of the camera is connected to the eyepiece of the trinocular tube. The quality of the image of the fluorescence domain can be controlled and improved using an automatic gain control. Video camera, monitor, and video tape recorder were interfaced to the surface balance for recording images of monolayer domains for subsequent analysis. The domain images can be analyzed using the menu-driven software (Jandel Scientific, JAVA, Corte Madera, CA) in combination with image-grabber board (Truevision, TARGA-M8), a digital VHS video recorder (JVC, HR-D700V, Japan), and monochromatic monitor (Panasonic, W-V54-10, Yokohama, Japan).

3.5 Additional Accessories:

The trough is contained inside a plastic enclosure. The dimensions of the enclosure are 70 x 45 x 42 cm. The distance between the trough and the top of the plastic enclosure is 24 cm. The enclosure provides the following:

1) Minimization of the air turbulence
2) Minimization of contamination by air borne impurities.
3) Minimization of the heat losses, and thus maintainance of constant temperature.
4) Minimization of the rate of evaporation of the subphase. This will improve surface tension measurements.

The whole unit of the surface balance is located on a large granite base. The base is in turn mounted on a vibration isolation system. See Fig. 3.4.

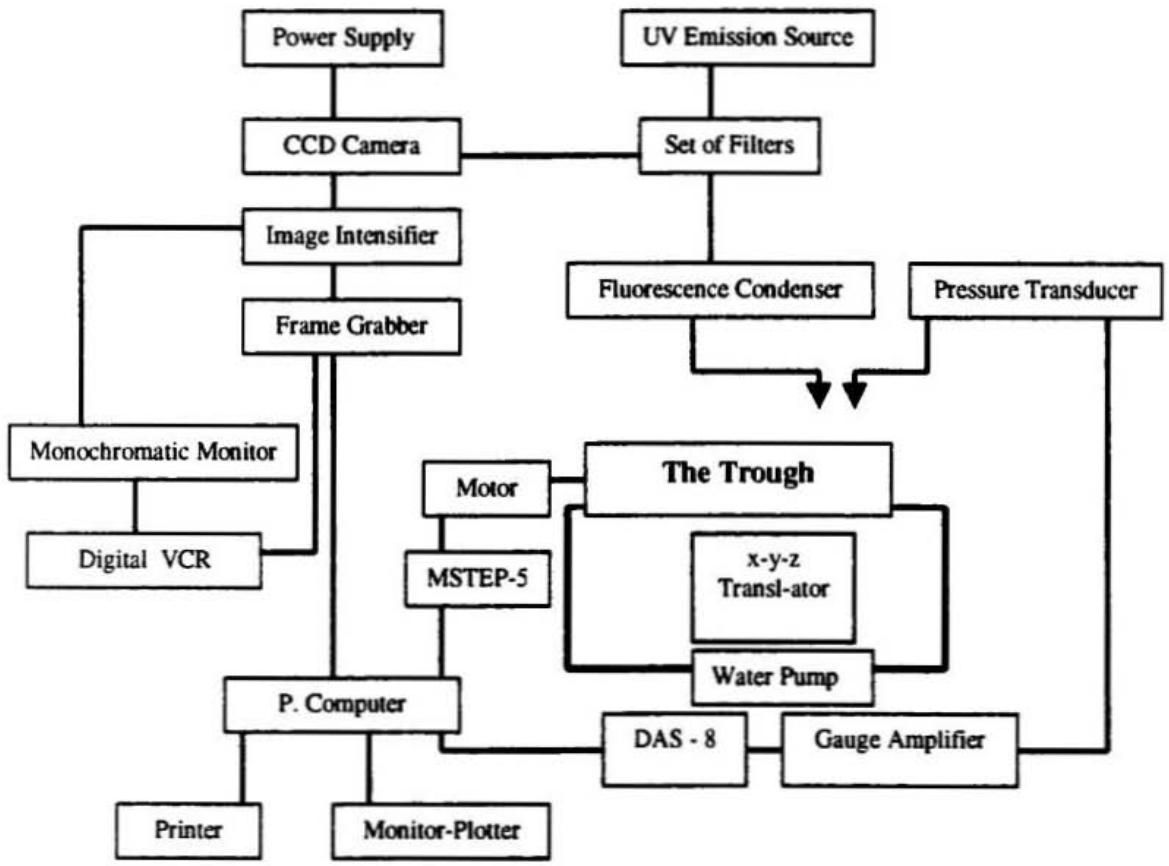

Fig. 3.3: Illustration for the block diagram of the Epifluorescence surface balance. Redrawn from [7].

3.6 Improvements and Amendments:

Some modifications have been introduced to the existing surface balance. To utilize the balance at different temperatures, it should be equipped with a temperature measuring and controlling system. To achieve this a set of twelve thermocouples has been introduced to the unit. The thermocouples are located at different sites inside the enclosure. In order to measure the subphase temperature four of the thermocouples are attached to the corners of the trough outside the area enclosed by the ribbon. Two are hung from above via a Teflon plate. The Teflon plate can be moved up and down. This can help in recording various temperatures at different locations at the middle of the trough. The remaining six thermocouples are distributed in different locations inside the enclosure and around the trough top part. This latter set enables monitoring of temperatures around the trough.

The set of the thermocouples is connected to a meter constructed at Memorial Technical Services Workshop.

In order to enhance the temperature uniformity inside the enclosure, two small fans (PP 401, DC 12V, 0.08 A, E157868, Taiwan) are located at different locations inside the enclosure. The fans are put off during image recording, so as to avoid the vibration caused by their motion.

The force transducer was found to be temperature sensitive. Increment by one degree of temperature has been found to raise the reading of the strain gauge by forty millivolts. To minimize the heat effect, and consequently reduce the heat contribution to the strain gauge reading, one can take the precaution of a) placing the air heater -in side the enclosure- away from the force transducer. b) Introducing a heat isolating enclosure

with dimensions 11.5 x 9 x 6 cm. to isolate the strain gauge unit from the surrounding heated air. In order to maintain equilibrium with the surrounding, the isolating enclosure of the strain gauge has a temperature controlling system (Omega Comp. CN 76000). The strain gauge is maintained at constant temperature, where it is calibrated, that is higher than the air temperature inside the enclosure.

One major problem that confronts a worker with the balance at higher temperatures is condensation of the subphase on the objective lens. This will result in preventing observation of the domain images. To eliminate the condensation on the lens a heater coil has been placed around the objective base. A cylindrical spool of Teflon makes a sliding friction fit around the barrel of the objective. A heater coil is wound on the spool. In order to avoid overheating the lens, the coil temperature is well controlled (Omega Comp. CN 76000). The coil will heat the base of the objective and the heat will transfer to the lens. The lens should be hotter than the subphase by 2-3 °C. This method eliminates the condensation problem.

Four pots with dimensions of 12 x 7 x 3 cm. filled with the subphase are located inside the enclosure. They help in saturating the air inside the enclosure. When saturation takes place, the evaporation of the subphase will be minimal.

In order to improve temperature measurements, the plastic enclosure was wrapped by aluminum foil. This method provides a constant temperature within ± 0.5 °C for the duration of the experiment run.

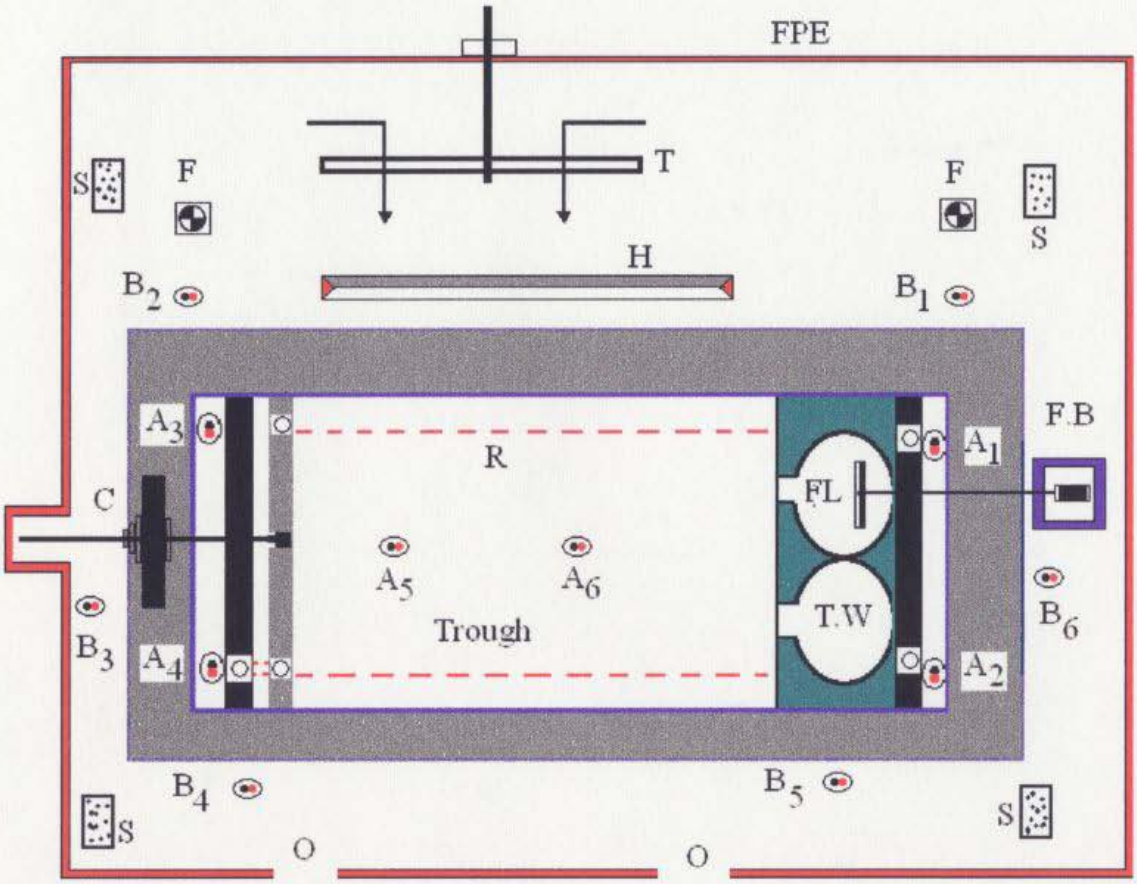

Fig.3.4: Top view of the trough of the Epifluorescence Surface Balance. The figure illustrates the introduced modifications. The thermocouples inside the trough (A's), the thermocouples outside the trough (B's), the foiled plastic enclosure (FPE), the Teflon plate (T), the heater (H), the fans (F), containers of the subphase (S), the crank shaft and the stepper motor (C), the ribbon (R), the foiled isolating box (FB), the flag (FL), and the twin piece (TW).

3.7 Materials preparation:

The solution of the monolayer film was prepared by dissolving 1,2-dipalmitoyl phosphatidylcholine (DPPC) and Dimyristoylphosphatidylcholine (DMPC) (Sigma Chemical Co., St. Louis, MO) into chloroform. A variety of solvents has been utilized in the published data; the effect of using different solvents -with different solvent effect- on isotherm of DPL monolayer has been reported in [94].

The molarity of the solution was measured utilizing the Bartlett phosphate assay method in the Biochemistry Department – Memorial University of Newfoundland. The dye probe is 1-Palmitoyl-2-{12-[(7-nitro-2-1, 3-benzoxadizole-4 yl) amino]dodecanoyl} phosphatidylcholine (NBD-PC) purchased from Avanti Polar Lipids (Pelham, Al). The dye was dissolved also in chloroform and its molarity was determined by the same assay method. The ratio of the dye probe to DPPC in the monolayer film was chosen to be 1%. It has been proven that the lesser the concentration of the dye probe in the monolayer, the lesser the perturbation to isotherms.

The subphase was prepared by dissolving 8.779 grams (0.15 M) NaCl in one liter of double distilled water. A solution of permanganate was used for the second distillation of the distilled water.

CHAPTER FOUR

RESULTS AND DISCUSSION

4. RESULTS AND DISCUSSION

4.1 Surface Tension Measurements:

The first thermodynamical parameter that has been determined - utilizing the modified surface balance- was the surface tension of water. The introduced modifications to temperature-control system have enabled us to perform measurements of surface tension of water at different temperatures. The results obtained on the surface tension of water are in good agreement with the published ones. [83]. See Fig. 4.1. The plot provides useful information as regards the interfacial forces of water, even near the critical temperature (T_c). T_c for water can be determined easily by determining the point where the surface tension is zero - from the plot in Fig. 4.1.

The accuracy in our measurements for T_c for water has been found to be 8%, in a good agreement with the accuracy in the published data.

4.1.1 The Dependence of the Force Transducer on Temperature:

One of the problems which confronts the worker with the surface balance at higher degrees of temperature, is the temperature effect on the force transducer of the surface balance. The effect was studied and a calibration curve has been displayed in Fig. 4.2. It is clear that an increment in temperature by one degree raises the reading of the strain gauge by a mount of 15 millivolts. In order to get precise readings from the force transducer the heat effect should be eliminated. A conclusion was drawn that the force transducer should be heat-isolated. An isolating box with heat controlling system (Omega Comp. CN 76000) was constructed at Memorial University of Newfoundland -Technical Services Department- to avoid the misreading of the force transducer at higher temperatures. The box was later wrapped with foil to improve the heat isolation.

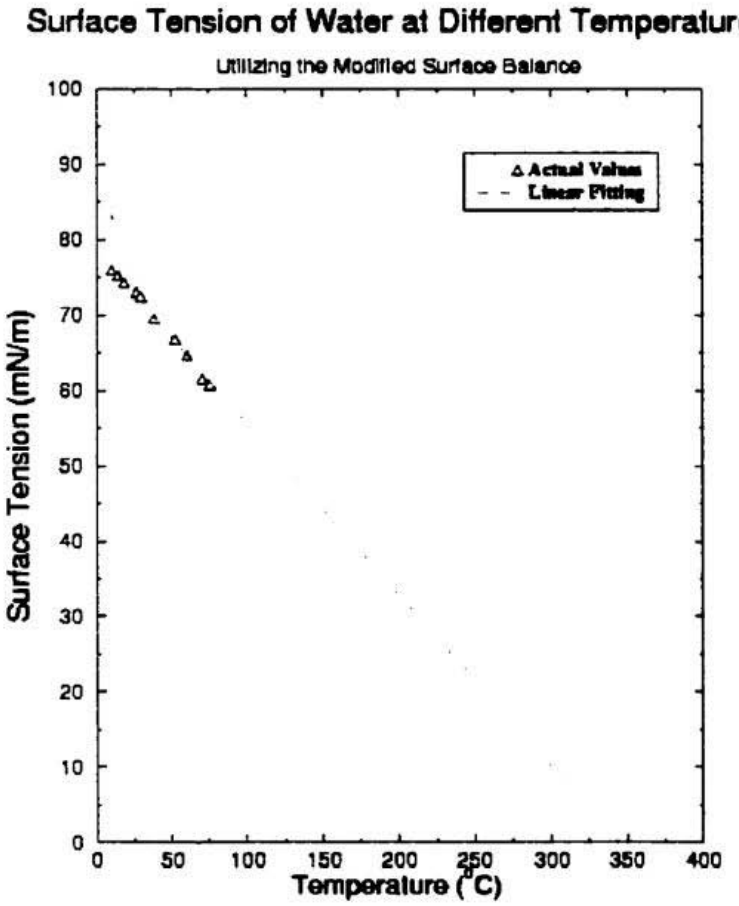

Fig. 4.1: The measurement of surface tension of water at different temperatures. Extrapolated fitting line intersects with the abscissa at $\gamma = 0$ indicating the critical temperature of water.

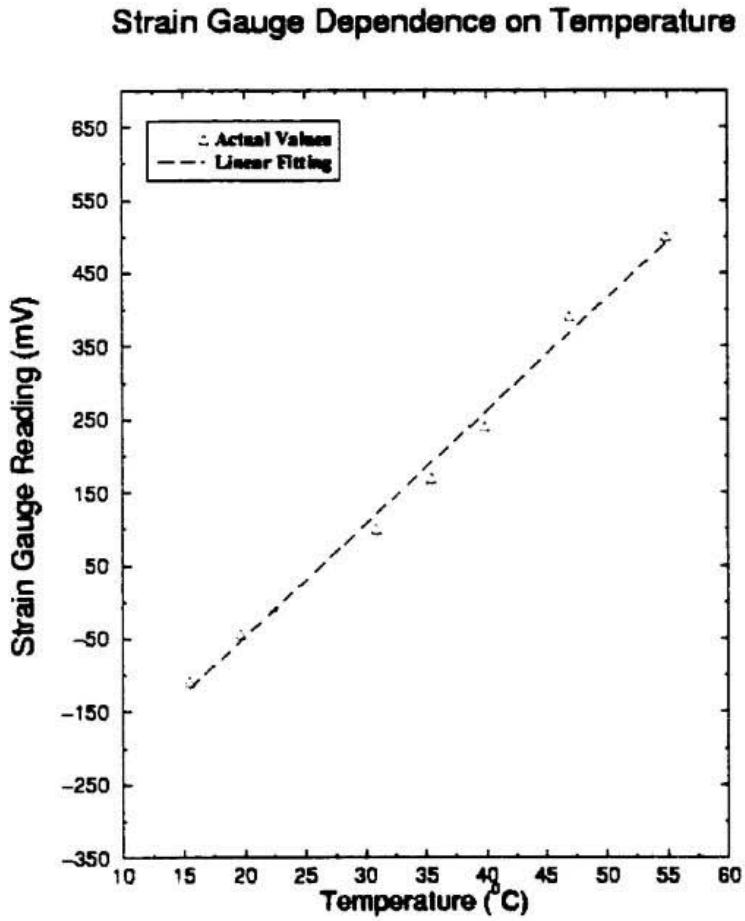

Fig. 4.2: Effect of temperature on force transducer.

4.2 π *vs.* A Isotherms of Phospholipid Monomolecular Films:

Utilizing the modified surface balance, the isotherms of the DPPC and DMPC at different temperatures have been measured. The procedures of preparing the monolayer film and controlling the temperature are explained below.

4.2.1 π *vs.* A Isotherms of DPPC:

In order to test the capability of our modifications on the surface balance, the isotherm of DPPC at room temperature was obtained first. After that isotherms of the same material were produced at different temperatures. A comparison between the findings in this study and what has been published in the literature is discussed.

4.2.2 The isotherm of DPPC at room temperature:

Fig. 4.3 illustrates the typical DPPC π-A isotherm at room temperature - 22 °C. The procedure for producing the isotherm starts by cleaning the trough - using methanol, distilled, and double distilled water- several times. After the cleaning, the film is deposited to the surface of the subphase in drops from a syringe. A waiting period of 30 minutes after the deposition was found to be sufficient for evaporation of the chloroform in which the DPPC had been dissolved. The compression was performed without waiting between compression steps. The speed of compression has been chosen to be 20 mm^2/second. The compression has been performed in 20 steps. The isotherm starts a "lift off", or a notable change in surface pressure above zero, at area per molecule of 80 $Å^2$/molecule. The surface pressure that corresponds to the main phase transition - LE to LC phase transition - was observed at 5.5 mN/m.; this is observed in the isotherm as a change in the slope of the curve. Moreover one can realize that the coexistence region is not perfectly horizontal.

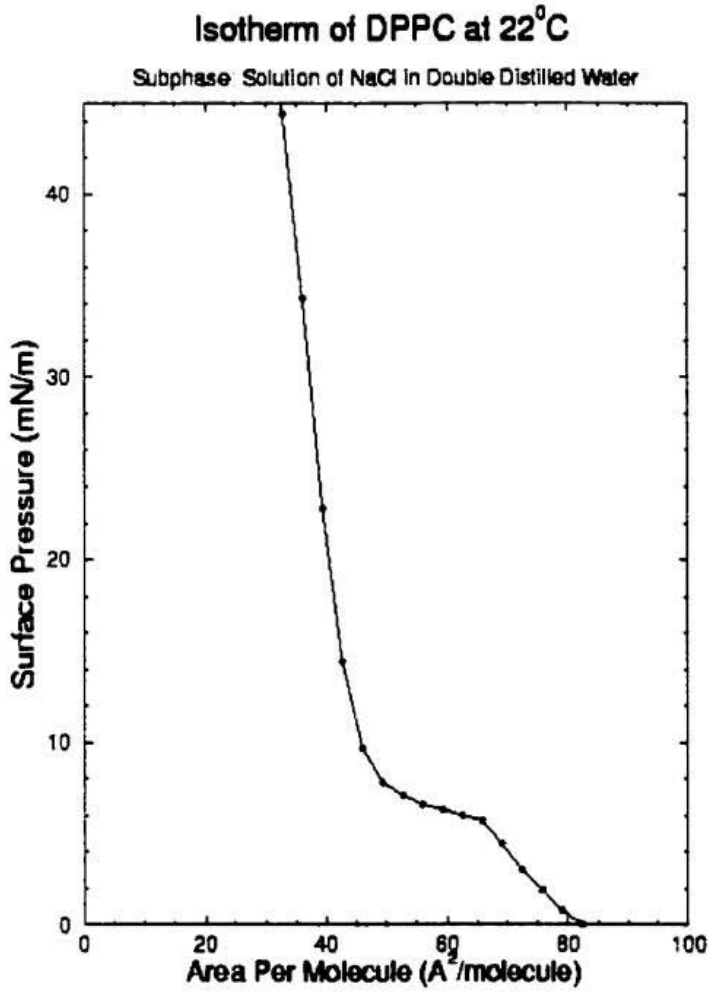

Fig. 4.3: π-A isotherm of DPPC at room temperature - 22 °C - obtained by utilizing the modified surface balance.

One of the possible reasons could be the presence of impurity despite careful trough cleaning.

4.2.3 Isotherms of DPPC at Different Temperatures than Room Temperature:

Several isotherms of the DPPC were obtained at different temperatures. The procedure for controlling the temperature of the surface balance during producing the isotherm is as follows: First the enclosure was heated for one hour by a heater and two fans inside the enclosure. The heater inside the enclosure can be set at a desired temperature. After one hour one can sense the uniformity of the heat distribution inside the enclosure by utilizing a set of twelve thermocouples. After the hour, the subphase was added to the trough and hot water at required temperature was circulated by the pumping system for another hour. This time was found to be sufficient to get the subphase at the desired temperature.

During the 30 minutes waiting period for the methanol evaporation, the heater and the fans were kept on to maintain the temperature constant while the hot water circulating pump was put off. Also a space heater was put outside near to the enclosure, utilized to minimize the heat losses from the inside of the enclosure. Tables 4.1, 4.2, and 4.3 illustrate temperature measurements during an experiment for obtaining isotherm at 30°C.

The measurements were registered at the beginning, after 30 minutes, and at the end of the experiment. ***A*** stands for the location of a certain thermocouple in side the trough i.e. thermocouple that measures the subphase temperatures while ***B*** stands for the location of a certain thermocouple on air around the trough i.e. thermocouple that measures the temperature of the trough surroundings. The locations are marked in black and red circles in Fig. 3.4.

Table **4.1**: Temperature measurement at the beginning of an experiment at 30 °C. **A** stands for location of thermocouple inside the trough. **B** stands for location of the thermocouple on air surrounding the trough.

A °C	$A_1 = 30.0$	$A_2 = 30.1$	$A_2 = 30.1$	$A_2 = 30.1$	$A_2 = 30.3$	$A_2 = 30.5$
B °C	$B_1 = 31.4$	$B_2 = 30.9$	$B_3 = 30.7$	$B_4 = 31$	$B_5 = 30.9$	$B_6 = 31.1$

Table **4.2**: Temperature measurement after 30 minutes from the beginning of an experiment at 30 °C. **A** stands for location of thermocouple inside the trough. **B** stands for location of the thermocouple on air surrounding the trough.

A °C	$A_1 = 30.2$	$A_2 = 30.2$	$A_3 = 30.3$	$A_4 = 30.4$	$A_5 = 30.2$	$A_6 = 30.4$
B °C	$B_1 = 31.4$	$B_2 = 31.4$	$B_3 = 31.2$	$B_4 = 32$	$B_5 = 30.7$	$B_6 = 31.4$

Table **4.3**: Temperature measurement at the end of an experiment at 30 °C. **A** stands for location of thermocouple inside the trough. **B** stands for location of the thermocouple on air surrounding the trough.

A °C	$A_1 = 30.1$	$A_2 = 30.1$	$A_3 = 30.4$	$A_4 = 30.3$	$A_5 = 30.3$	$A_6 = 30.2$
B °C	$B_1 = 31.4$	$B_2 = 30.7$	$B_3 = 30.9$	$B_4 = 32$	$B_5 = 30.9$	$B_6 = 31.1$

Temperature measurement was carried out throughout the experiment to ensure that the losses in temperature were minimal. From tables 4.1, 4.2, and 4.3 one can observe that the temperature is quite stable and uniform during the period of the experiment.

4.2.4 DPPC isotherm at 42 °C:

The isotherm at 42 °C is illustrated in Fig 4.4. The isotherm starts at 101 $Å^2$/molecule. The main phase transition has been observed to occur at 41 mN/m. One observation can be drawn from the isotherm at this temperature; that is the difficulty in determination of the exact value of the main phase transition point. A method has been followed to determine an approximate value. The slopes of the two parts of the isotherm - before and after the turning region- were drawn. The point of intersection of the two slopes has been chosen as the best point to account for the main phase transition [91]. Moreover one can observe the plateau at the surface pressure of 46 mN/m; most likely the film starts to breakup - "raft"- at this surface pressure [91].

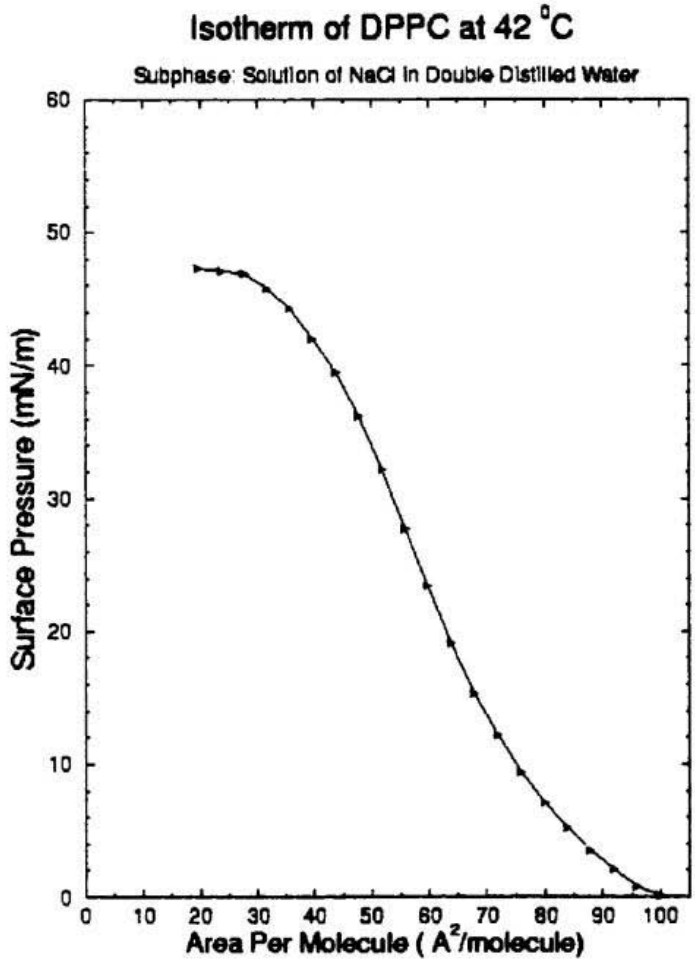

Fig. 4.4: π-A isotherm of DPPC at 42 °C - obtained by utilizing the modified surface balance.

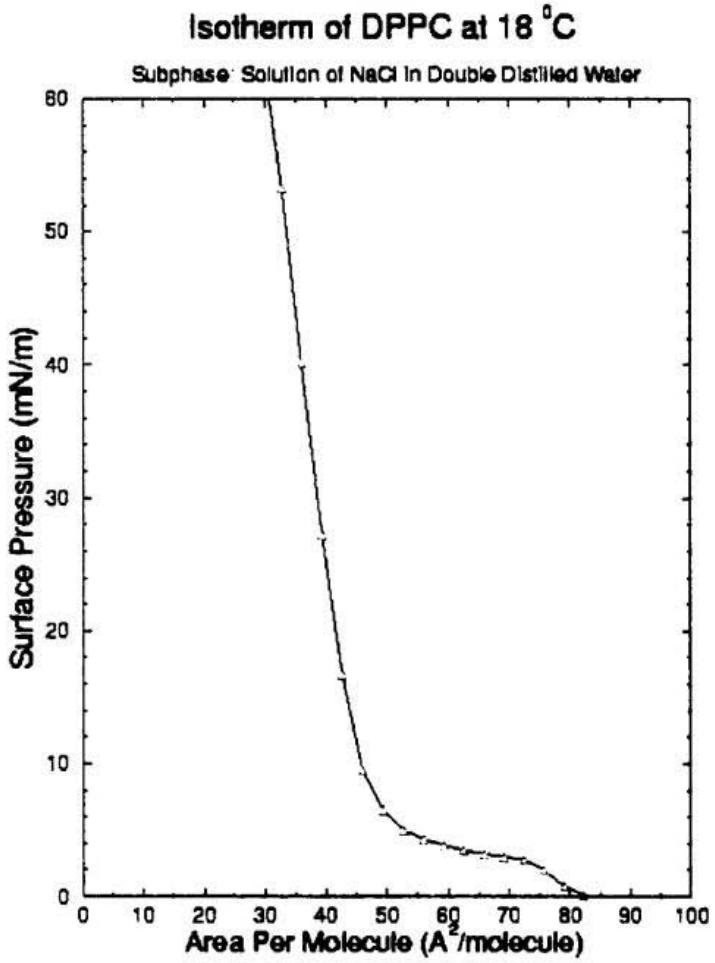

Fig. 4.5: π-A isotherm of DPPC at 18 °C - obtained by utilizing the modified surface balance.

4.2.5 DPPC isotherms at temperatures in the range from 14 °C to 42 °C:

Looking at the plot of all isotherms- Fig. 4.6, one can confirm the fact that as the temperature of the isotherm increases -from 14 °C to 42 °C- the surface pressure which corresponds to the main phase transition increases also. In addition the area per molecule where each isotherm starts (" lift off") increases also. At higher temperature the isotherms no longer clearly show LE/LC coexistence. Here the visualization can serve as good tool to uncover the coexistence region. Crossing of the isotherms at higher pressures indicates the difficulty of accurate measurements with the steep slopes.

DPPC isotherms at different temperatures have been reported in the literature [60] [3][4][5][42][43]. The isotherms that have been reported here are in good agreements with those that have been published. One notable difference between the isotherms constructed in this study and those that have been published is the determination of the area per molecule where the isotherm starts. In this study the concentration of the sample of the DPPC has been determined by the Bartlett phosphate assay method. The precise concentration yields a precise determination for the area per molecule. Thus the area per molecule is well determined here.

The isotherms confirm the fact that below 14 °C the film is in LC phase while above 42 °C the film is totally in LE phase.

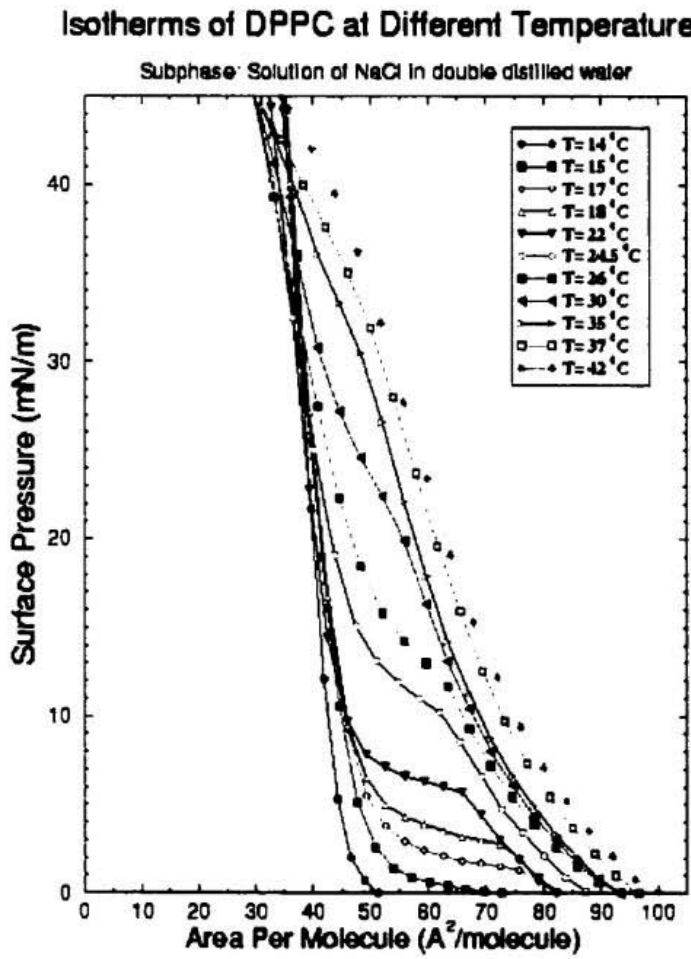

Fig. 4.6: π-A isotherms of DPPC at different temperatures obtained by utilizing the modified surface balance.

4.2.6 π *vs.* T:

The relation between the isotherm temperature and the surface pressure that corresponds to the onset of the LE/LC phase transition has been investigated in this study. Fig. 4.7 illustrates that relation with a quadratic fit to the data in excellent agreement with the published results [4].

In order to calculate the latent heat of the main phase transition a linear fit to these data was forced despite the obvious non-linearity, giving a slope of 1.7 mN/m.°C for an average value of $\frac{d\pi_c}{dT}$. This may be compared to a reported [3] value of 1.3 mN/m.°C. In addition the discrepancy in the values may be due to the method of determining the point of onset of the main phase transition, which has been extracted from the isotherms by intersecting the slopes.

4.2.7 A_t *vs.* T:

Fig. 4.8 displays the relation between the area per molecule at the onset of the main phase transition -A_t- and the temperature of the isotherm. The relation has been found to be linear. The slope of the fitting line is – 1.27 Å^2/molecule.°C.

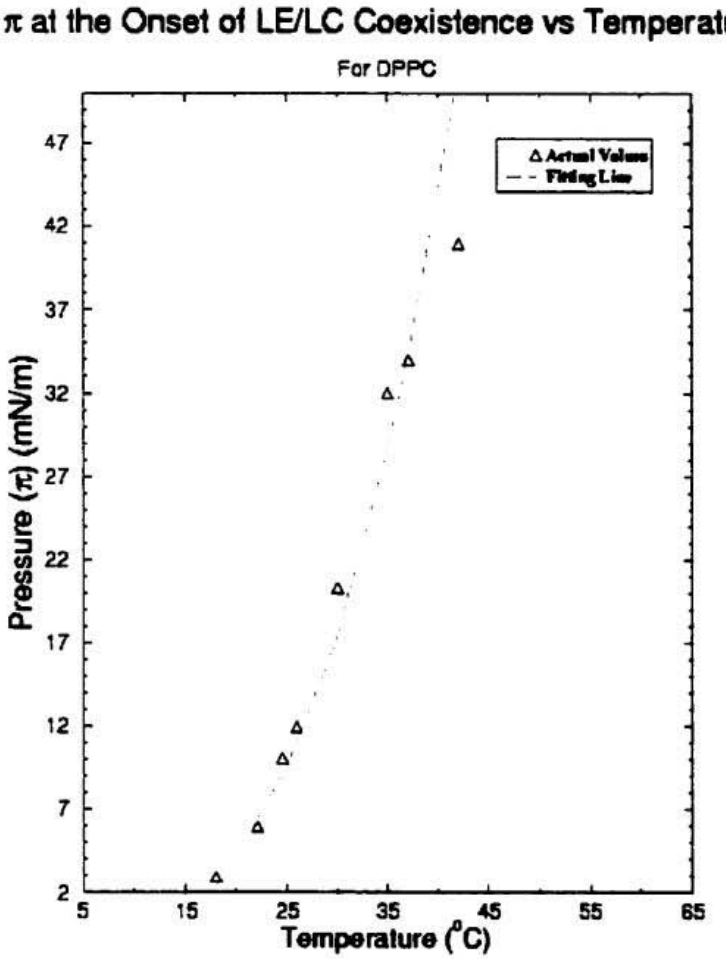

Fig. 4.7: Surface pressure at the onset of the LE/LC DPPC phase transition as function of isotherm temperature.

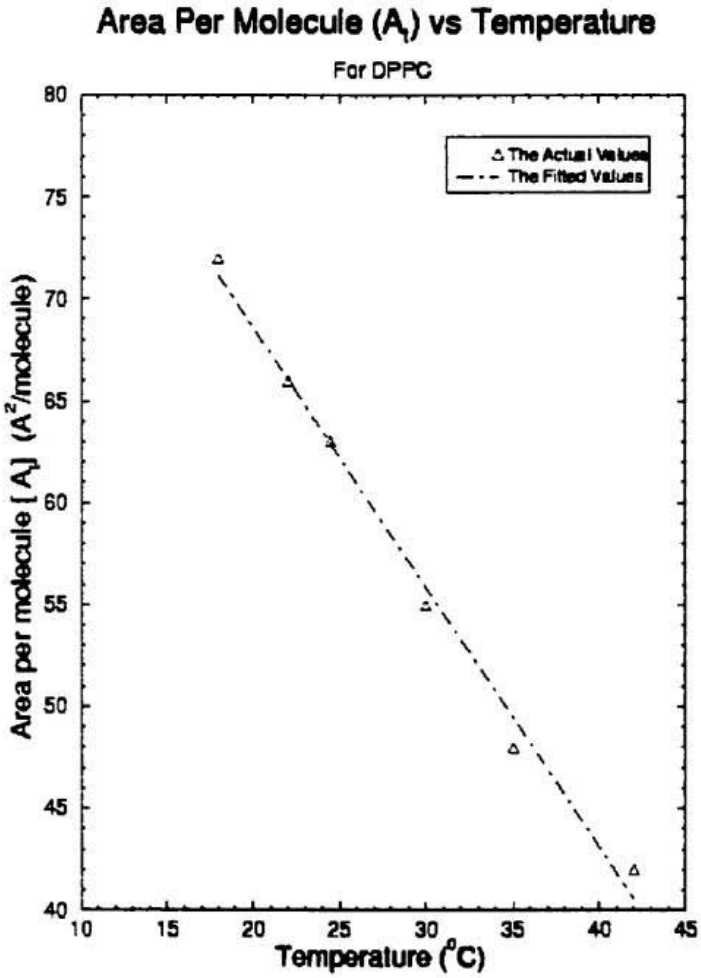

Fig. 4.8: The relation between area per molecule at the onset of LE/LC -A_t- of DPPC phase transition and isotherm temperature.

4.3 DMPC isotherms at different temperatures in the range from 6 °C to 23.3 °C:

Fig. 4.9 illustrates the isotherms of DMPC at different temperatures starting from 6 °C to 23.3 °C.

The same type of observation that has been observed on the DPPC isotherms at different temperatures is seen here. It is very difficult to determine exactly the point where the phase transition occurs. The method of slopes intersection has been applied for that determination. According to the literature [6] the DMPC film at temperature above its melting chain temperature -23 °C- is totally in LE phase, this can be observed from Fig. 4.9.

The isotherms are in good agreement with those obtained by [42]. The area per molecule is slightly different for the reason stated previously.

From Fig. 4.9 one can observe that the LE/LC coexistence region has disappeared at temperature of 23.3 °C. That confirms the fact that the film will be totally LE above this temperature.

4.3.1 π *vs.* T:

Fig. 4.10 displays the plot of the relation between the surface pressure that corresponds to the onset of the LE/LC coexistence region and the isotherm temperature. In contrast to DPPC plot this one is linear with slope 1.9 mN/m.°C.

4.3.2 A_t *vs.* T:

Fig. 4.11 displays a plot of the relation between the area per molecule that corresponds to the onset of the LE/LC coexistence region - A_t - and the temperature of DMPC isotherm. The linear fit has slope – 1.56 $Å^2$/molecule.°C.

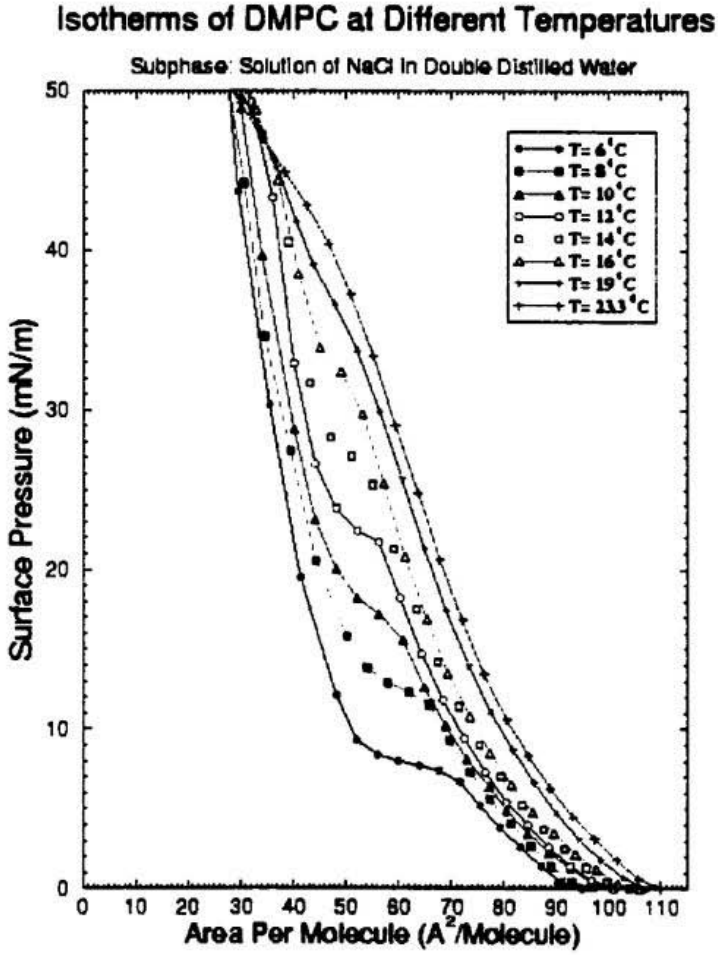

Fig. 4.9: π-A isotherm of DMPC at different temperatures. Produced by utilizing the modified surface balance.

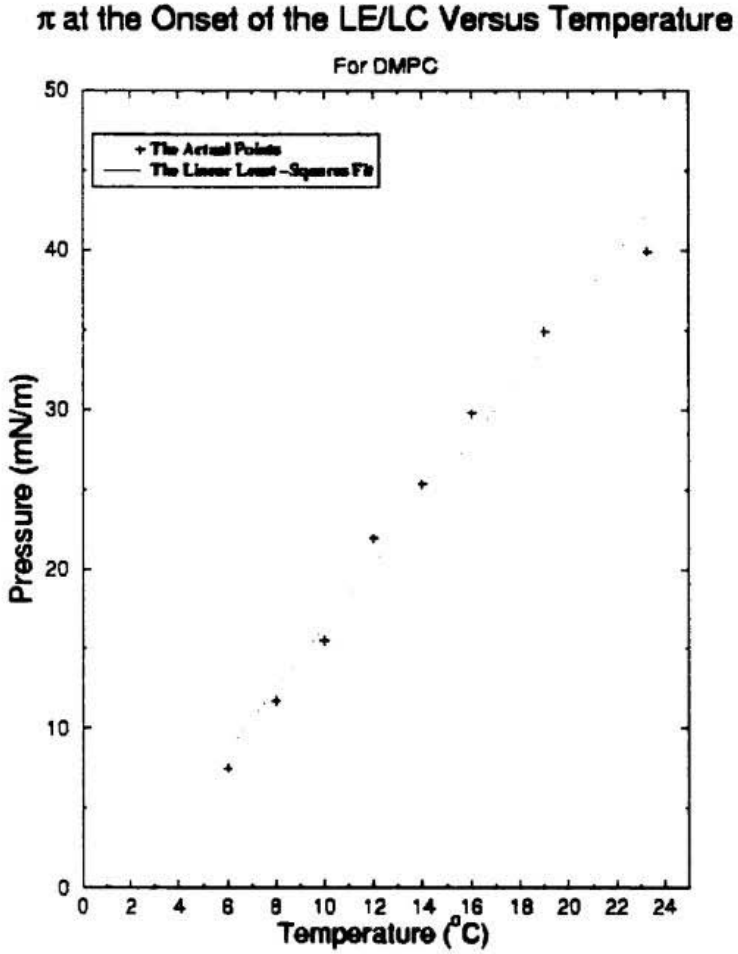

Fig. 4.10: The relation between the surface pressure at DMPC main phase transition and the isotherm temperature.

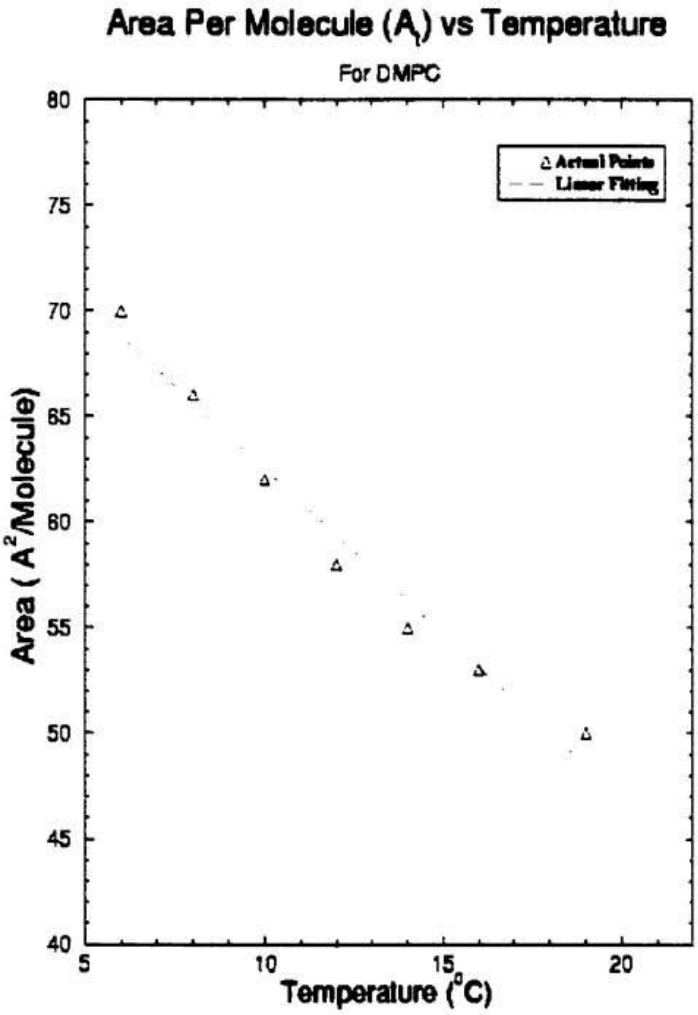

Fig. 4.11: The relation between the area per molecule at DMPC main phase transition and the isotherm temperature.

4.4 Latent Heat of Transition:

4.4.1 For DPPC:

The latent heat of the main phase transition has been calculated at different temperatures using equation 2.5. The relation between the latent heat of the main phase transition - Q_{main} - and the temperature of the isotherm has been plotted in Fig. 4.12. The relation has been found to be linear. As the temperature increases Q_{main} has been found to decrease.

4.4.2 For DMPC:

By utilizing the same method the latent heat of the main phase transition for DMPC film has been calculated at different temperatures. The relation between Q_{main} and the temperature of the isotherm has been plotted in Fig. 4.12. The relation has been found to be linear. As the temperature increases, Q_{main} has been found to decrease.

The calculation of the latent heat of the main phase transition was based on the measurements of the length of LE/LC coexistence region and calculation of $\frac{d\pi_c}{dT}$ (the slope of the plots in Figs. 4.7 for DPPC and 4.10 for DMPC). The length of that region has been measured for both DPPC and DPMC from their isotherms at different temperatures in Figs. 4.6 and 4.9 respectively. There are some uncertainties involved in determining the limits of the coexistence area and in calculating $\frac{d\pi_c}{dT}$. Those uncertainties can lead to a slight difference in the exact values of the latent heat of the main transition for both DPPC and DMPC, even though the general behavior is still maintained.

4.4.3 Comparison between the latent heat at main phase transition of DPPC and DMPC:

Fig. 4.12 displays a comparison between the plots of Q_{main} versus temperature for both DPPC and DMPC. The slope of the two fitting lines should be the same in the ideal case.

A recent comprehensive and useful review of monolayers [92] includes results on latent heat and entropy changes in phase transitions, reporting that monolayers formed by molecules differing only in chain length experience the same sequence of phase transition - change in latent heat and entropy-, but at individual fixed temperatures. In general DMPC orders at lower temperature and with smaller latent heat than DPPC.

According to the published data the latent heat at main phase transition of DPPC and DMPC bilayers are 26.9 K.J/mol. at 41.05 °C and 21.1 K.J/mol. at 23.2 °C respectively [26].

The latent heat at main phase transition for DPPC monolayer at 41 °C was found to be 22 K.J/mol. while that for DMPC at 23 °C was found to be 15 K.J/mol. One can note that the latent heat of the main phase transition for both monolayer and bilayer of DPPC and DMPC are comparable.

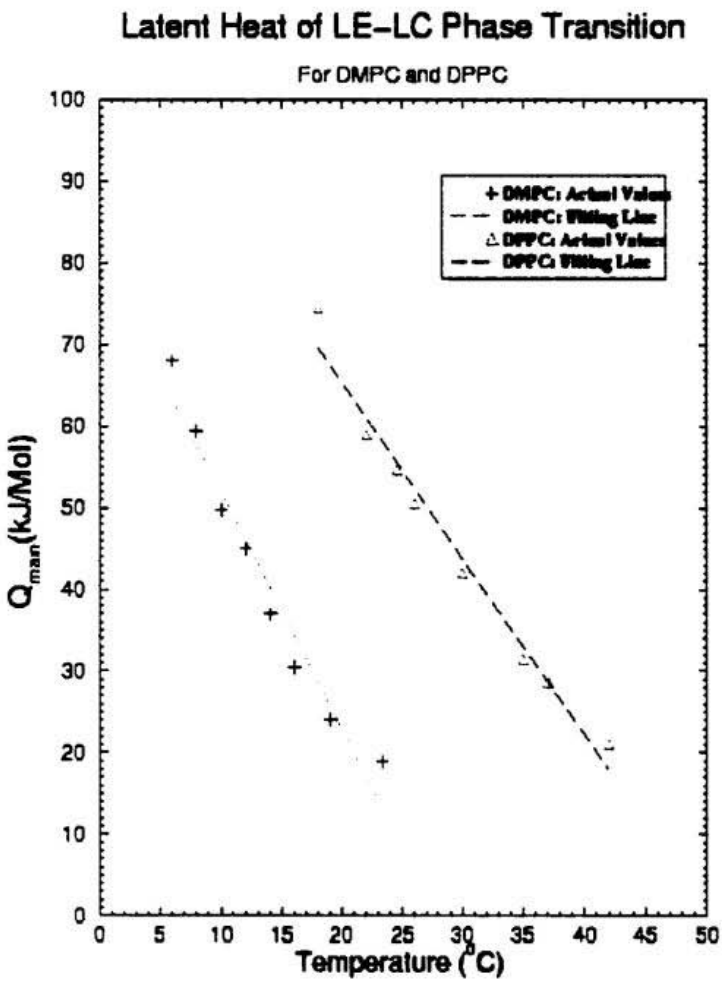

Fig. 4.12: Comparison between the plots of latent heat (Q_{main}) *versus* temperature of DPPC and DMPC.

4.5 DPPC Domain Visualization at 18 °C:

4.5.1 Images at different surface pressures:

Many published articles have revealed DPPC domains in the coexistence region of the isotherm [8][9][80]. In this study the epifluorescence arrangement has been utilized to visualize DPPC domains. The modifications that have been introduced to the existing balance have enhanced the temperature control. DPPC domains at temperature of 18 °C were visualized at different surface pressure. Figures from 4.13 to 4.17 illustrate the growth and progression of the domain shapes and sizes through the coexistence region.

The dark domains have been observed to grow out of the fluorescent background at surface pressure of 2.5 mN/m at area per molecule of 71.2 ± 3 $Å^2$/molecule. See Fig. 4.13A.

The speed of compression was 20 mm^2/sec. At each surface pressure a 2-minutes waiting time was introduced before recording was taken. Recording time was always about two minutes.

Initially, domains appear completely round with the resolution of our microscope. It is not clear whether this is due to the limits in the resolution or if it is the case in reality. As the compression progresses the domains have been found to grow with finger like projection. Fig. 4.13B illustrates the increase in size for the next surface pressure π = 2.6 mN/m and at area per molecule A = 71.13 ± 3 $Å^2$/molecule.

As the surface pressure increases the domain size increases also. See Fig. 4.14A at surface pressure of 2.7 mN/m and at area per molecule of A = 71.1±3 $Å^2$/molecule. At surface pressure of 2.8 mN/m and area per molecule A = 71.1±3 $Å^2$/molecule image was

recorded and illustrated in Fig. 4.14B. At surface pressure of 2.9 mN/m and area per molecule A= 71.0 ± 3 $Å^2$/molecule, the domains were imaged and illustrated in Fig. 4.15A.

Figure 4.15B illustrates the domain size and shape at surface pressure 3.1 mN/m and area per molecule 70.7 ±3 $Å^2$/molecule. Some small kidney bean shapes started to appear at this surface pressure.

The more regular shape of the domains was observed at surface pressure of 3.7 mN/m and area per molecule 70.3±3 $Å^2$/molecule. The domains at this surface pressure are homogeneous distributed in shape in agreement with the published data [80].

The predominant domain shape at this surface pressure -3.7 mN/m- is kidney bean with distinct cavity. That can be seen at Fig. 4.16A. The domains were found to be asymmetric. If the bean is oriented with its cavity facing upwards, the left lobe has flattened edge. This observation is in an excellent agreement with Flörsheimer, Möhwald, and Cary W. McConlogue findings [8]. McConlogue has pointed that DPPC domains are chiral; in this study the DPPC chirality has been observed.

Domains were found to grow even beyond the horizontal plateau – coexistence – region up to π =5.2 mN/m

According to McConlogue observations, the flattened edge of the kidney bean plays a role in domain growth at higher pressure (i.e. in more condensed films)[35][36]. Fig. 4.16B illustrates the domain at surface pressure π = 5.2 mN/m and area per molecule of 68.6 ± 3 $Å^2$/molecule where kidney beans start to touch each other.

Upon further compression the beans fused together; this is illustrated in Fig 4.17A at surface pressure π=12.4 mN/m and area per molecule A= 61.4 ± 3 $Å^2$/molecule. This

can serve as an indication for the end of the LE/LC coexistence region and beginning of the totally LC phase.

At the surface pressure of 23.4 mN/m and area per molecule of 50.4±3 $Å^2$/molecule the film is totally in solid phase, see Fig. 4.17B. The film in this phase has been observed to be stiff and very hard to move. At higher surface pressure - in our case 23.4 mN/m - the dark domains become very small in size. The eyepiece has been utilized to see the morphology of the film at higher pressure. This is an indication for the complete solidification of the film. The recording of the visualization is very difficult at this stage due to the lower fluorescence observed from the monolayer. According to K. Nag, the fluorescent probe suffers self-quenching at higher surface pressure regions. At 18 °C, the highest surface pressure that we could capture domain image is 23.4 mN/m. After that the image quality was found to be very poor in contrast.

The images of the domains at this temperature have been visualized utilizing an objective lens with magnification 50X. To compare the domain sizes of those captured by an objective of magnification 40X with those captured by 50X, the sizes of the latter have been multiplied by a factor of 0.8.

To find the locations of the points where compression has been stopped for images visualization and recording refer to the isotherm in Fig. 4.5. The surface pressure and the area per molecule where those recordings are made are presented below each domain image.

4.5.2 The fraction of liquid condensed phase as a function of surface pressure:

The fraction of the liquid condensed phase at a given surface pressure or area per molecule can be determined. In this study, the domains of the DPPC film at 18 °C have

been analyzed. The procedure of determining the liquid condensed fraction has been achieved by utilizing image analysis software. In this procedure a certain area can be demarcated by the mouse of the computer as the area of interest (AOI). The software will calculate the sizes of the dark domains inside the AOI. The total area of the dark domains will be calculated and the software will determine the fraction of the dark area -liquid condensed-. The determination of the size of the dark area starts by circling the area by a line. The procedure involves some uncertainties in determining the exact area, especially when the image is not clear enough in the monitor.

The above procedure was followed in determining the fraction of the liquid condensed at different surface pressures at temperature of 18 °C. Illustration of the fraction of the liquid condensed as function of the surface pressure is presented in Fig. 4.18. One can observe as the surface pressure increases the fraction of the liquid condensed increases also. A good agreement between findings in this study and K. Nag finding has been observed. [25].

4.5.3 The fraction of liquid condensed phase as a function of area per molecule:

Fig. 4.19 illustrates the fraction of the liquid condensed for DPPC monolayer as function of the area per molecule. One can deduce that the film is in total solid state when the area per molecule reaches about 46 $Å^2$/molecule. This in good agreement with the theory that predicts the cross sectional area of DPPC chains has value of 40 $Å^2$.

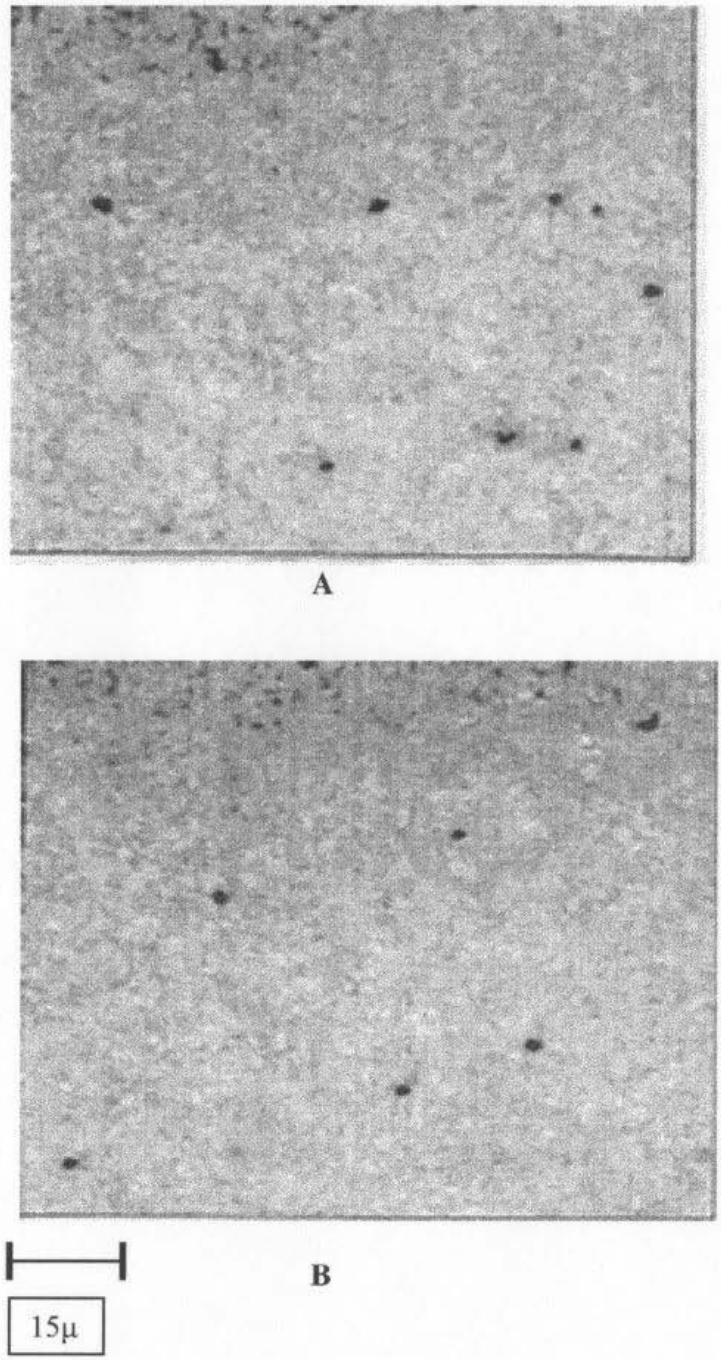

Fig. 4.13: DPPC domain shapes and size at 18 °C as the compression progresses.

A: at $\pi = 2.5$ mN/m. B: at $\pi = 2.6$ mN/m.

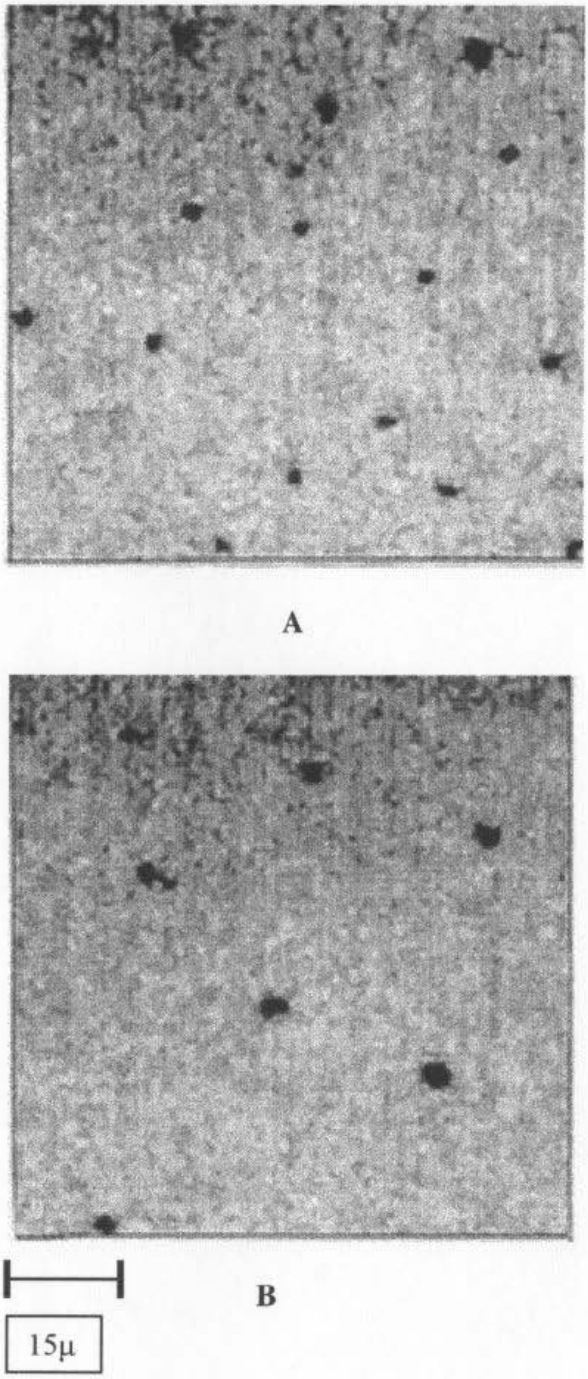

Fig. 4.14: DPPC domain shapes and size at 18 °C as the compression progresses.

A: at π =2.7 mN/m. B: at π = 2.8 mN/m.

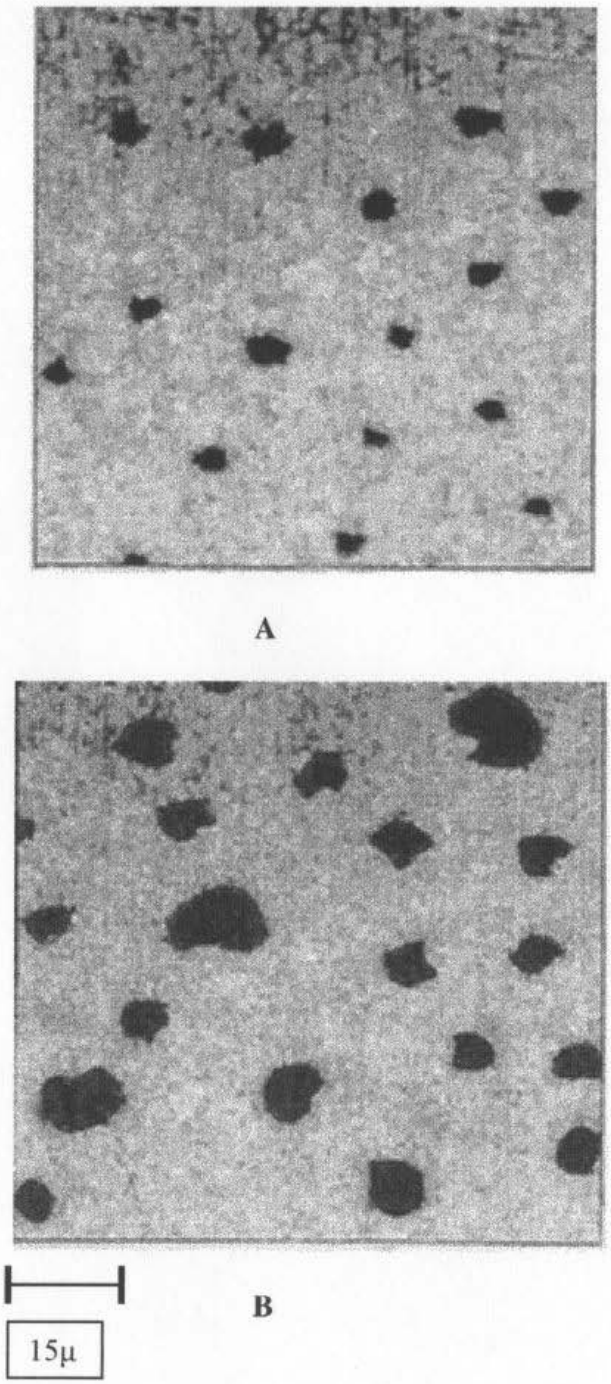

Fig. 4.15: DPPC domain shapes and size at 18 °C as the compression progresses.

A: at $\pi = 2.9$ mN/m. B: at $\pi = 3.1$ mN/m.

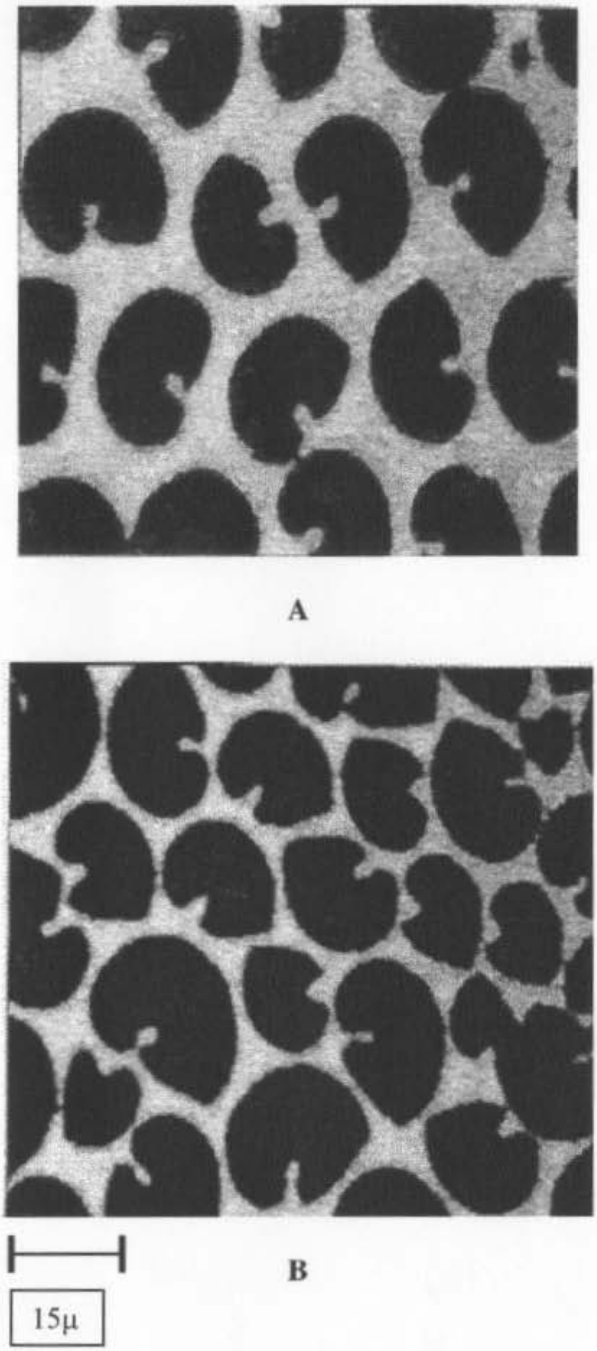

Fig. 4.16: DPPC domains shape and size at 18 °C as the compression progresses.

A: at π =3.7 mN/m. B: at π = 5.2 mN/m.

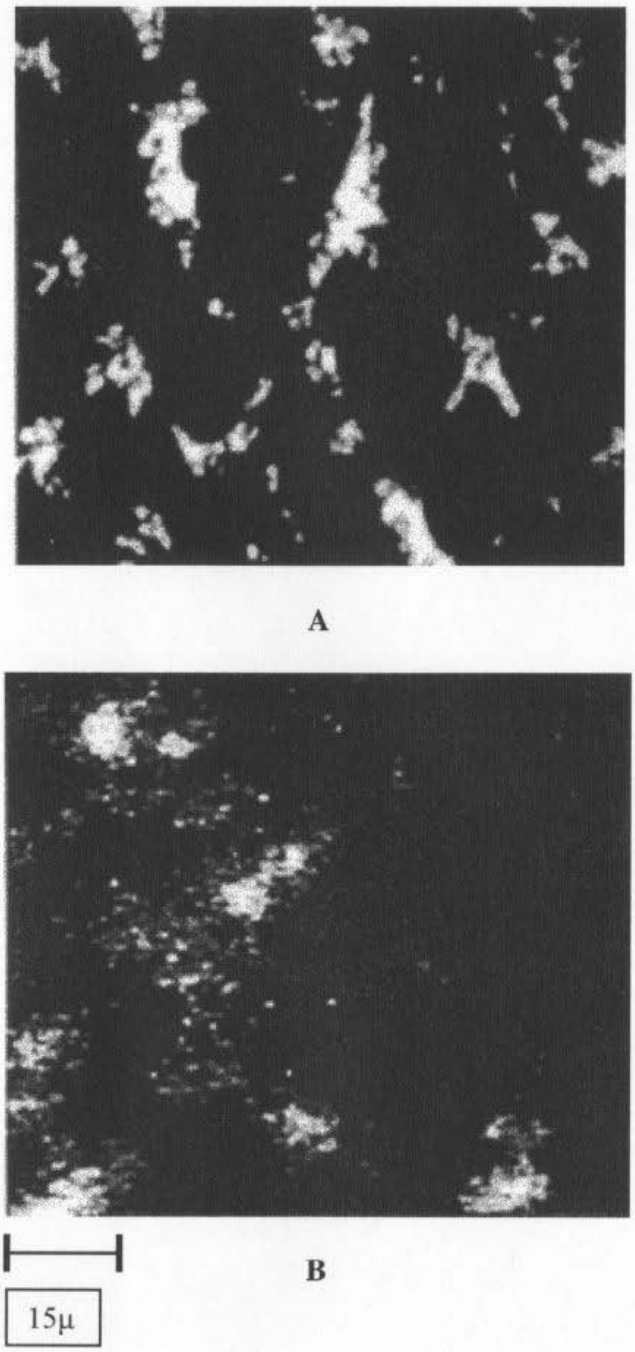

Fig. 4.17: DPPC domains shape and size at 18 °C as the compression progresses.

A: at π =12.4 mN/m. B: at π = 23.4 mN/m.

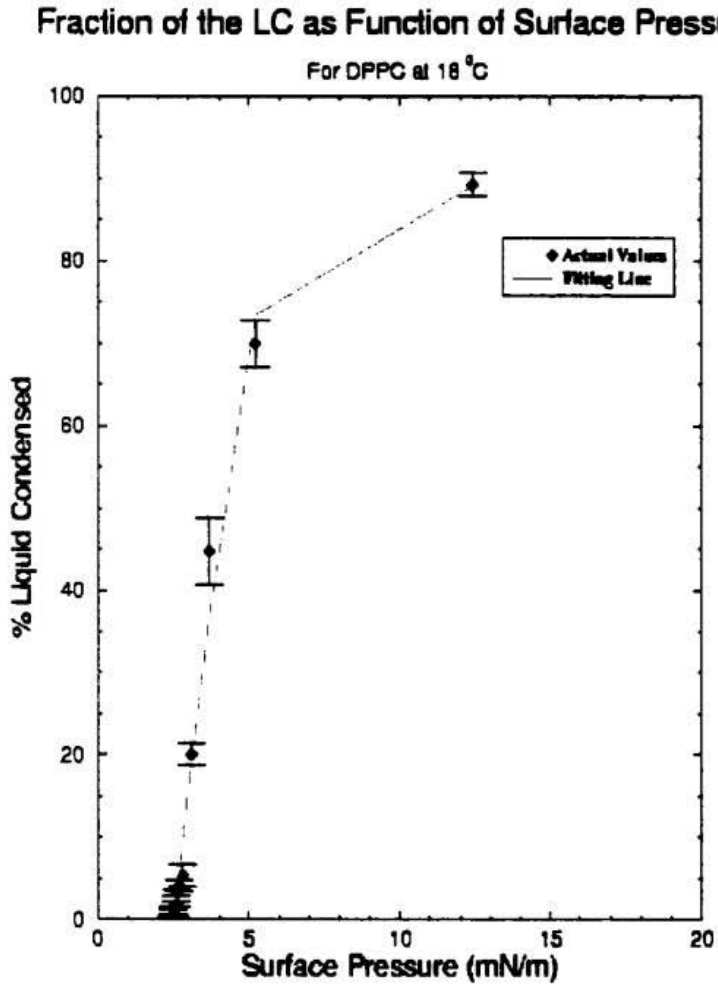

Fig. 4.18: The fraction of the liquid condensed phase as function of the surface pressure. The line is a quadratic fitting line.

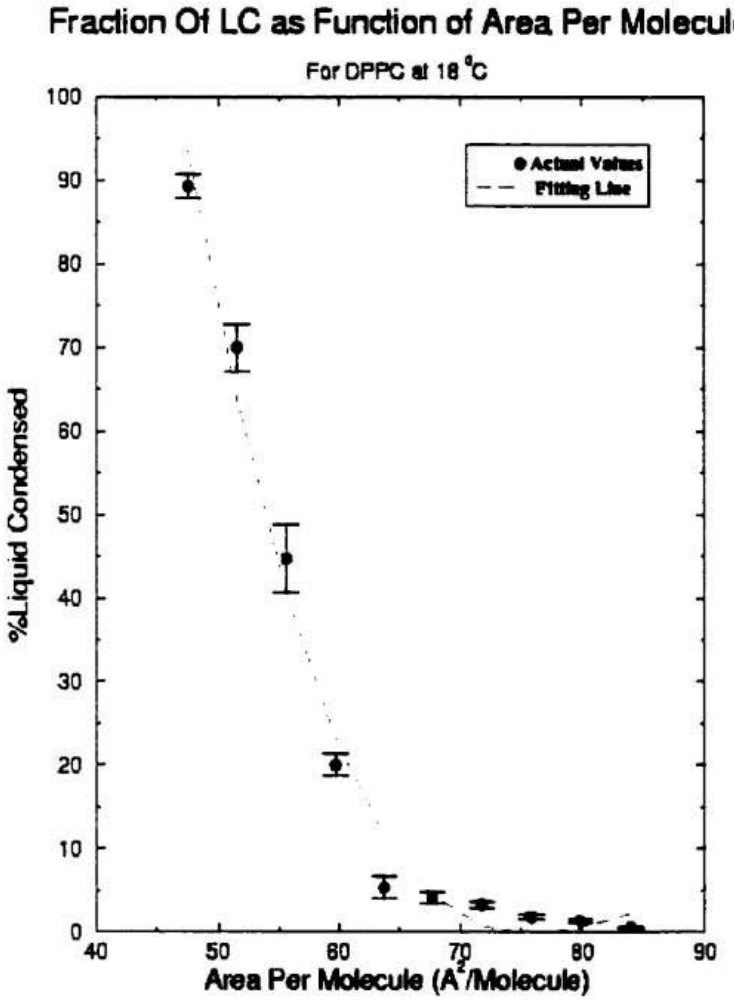

Fig. 4.19: The fraction of the liquid condensed phase as function of area per molecule. The line is a third degree fitting line.

4.6 Diversity of DPPC Domain Shapes in the Coexistence Region:

In this study some DPPC domains with different shapes from the fundamental kidney bean shape have been reported. By the end of the coexistence region of DPPC film at 18 °C at surface pressure of 5.2 mN/m, kidney beans, S-like, multilobed, and circular domains have been visualized. The film has been compressed at 20 mm^2/molecule with two minutes waiting time in between compressions. At surface pressure of 5.2 mN/m 15 minutes waiting time was introduced. Fig.4.24 illustrates the distribution of DPPC domain shapes at this surface pressure. The predominant shape has been found to be kidney beans, then S-like, circular, and multilobed respectively. McConlogue etal have reported similar shapes [8]. They follow different experimental protocol by aging the film from 8 to 10 hours. McConlogue has presented a model that explains the development of the domain shapes. The principal idea beyond that model is that the nub in DPPC domain has originated from the flat edge of the kidney bean and progresses to S-like shape and then to the multilobe shape. Moreover he has proposed that the projection will develop and eventually result in the formation of the domain shape presented in Figs.4.20B, 4.22A. We report visualization of the nub of the domain as progressing in Fig.4.23A. Utilizing McConlogue model one can explain the progress of the domain shape from kidney bean to multilobe domain. Fig. 4.20A illustrates the kidney bean domain with its flat edge extending into the interior of the cavity, in agreement with the findings of McConlogue. He has also proposed that some beans can develop a nub inside the cavity. In Fig. 4.22B some beans with a cavity nub have been presented.

McConlogue has not observed any circular domains when compressing the film. Instead he has reported some circular domains when expanding a compressed DPPC film. In this study some circular domains have been visualized when compressing the film at 20 mm^2/molecule at surface pressure 5.2 mN/m. According to his model the circular domains result from the fact that the flattened edge moves around to the interior of the domain cavity. Some of the domains exhibit self-fusion creating a pocket in the domain. The pocket slowly moves towards the center of the domains and the domain itself becomes circular. Illustration of that situation is presented in Fig.4.21A.

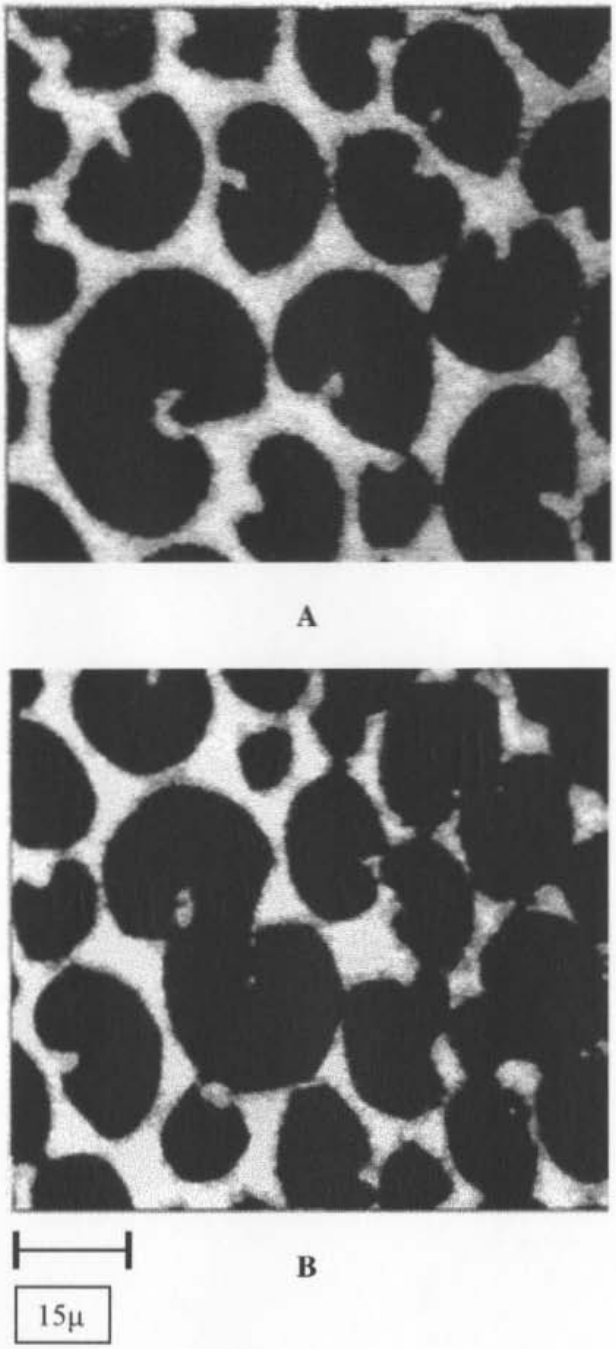

Fig. 4.20: DPPC domain shapes at 18 °C at π = 5.2 mN/m. A: Kidney beans with projection inside the cavity. B: S-like domain.

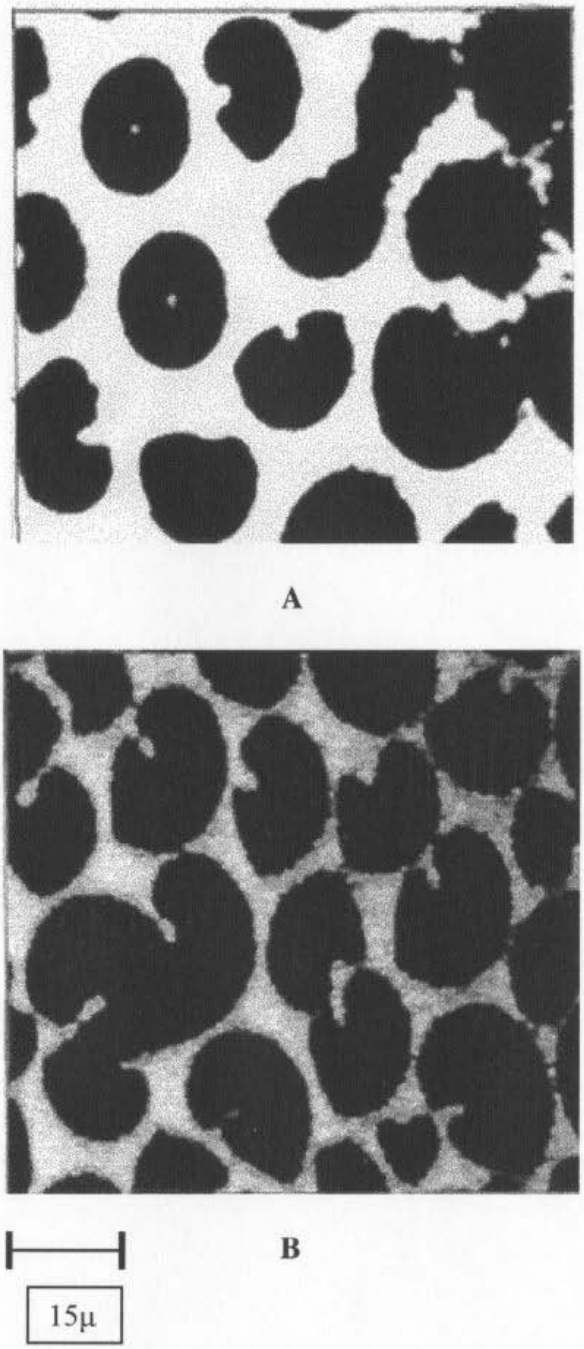

Fig. 4.21: DPPC domain shapes at 18 °C at π = 5.2 mN/m. A: Circular domains. B: Bilobe domain.

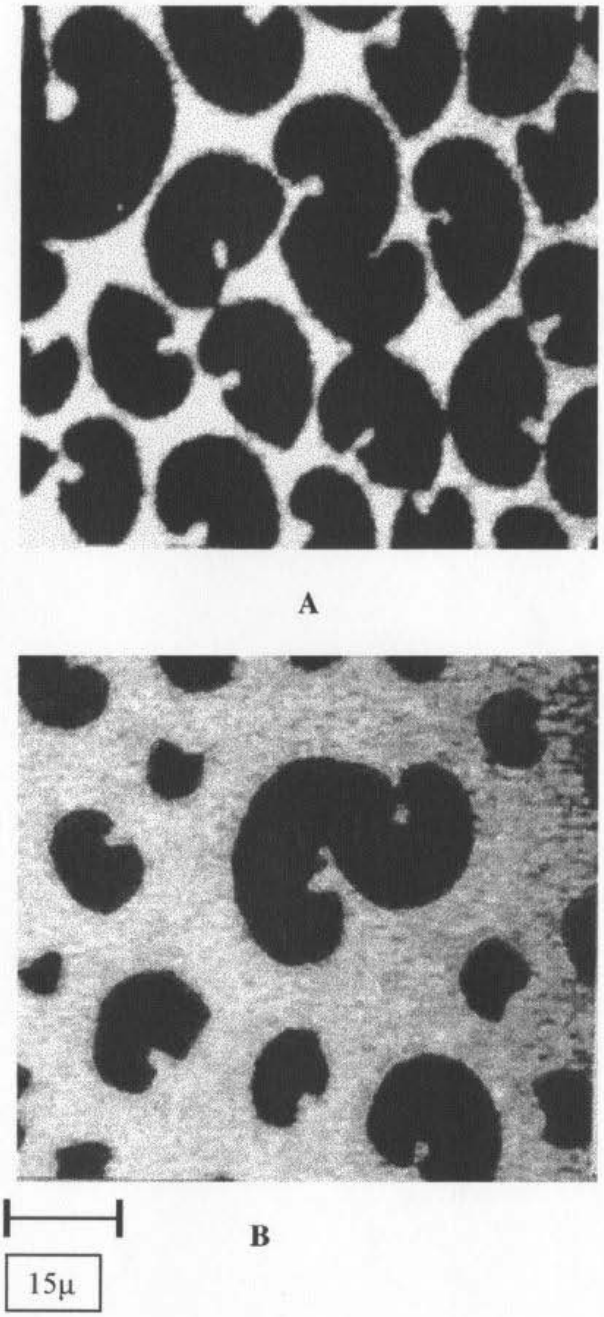

Fig. 4.22: DPPC domain shapes at 18 °C at π = 5.2 mN/m.

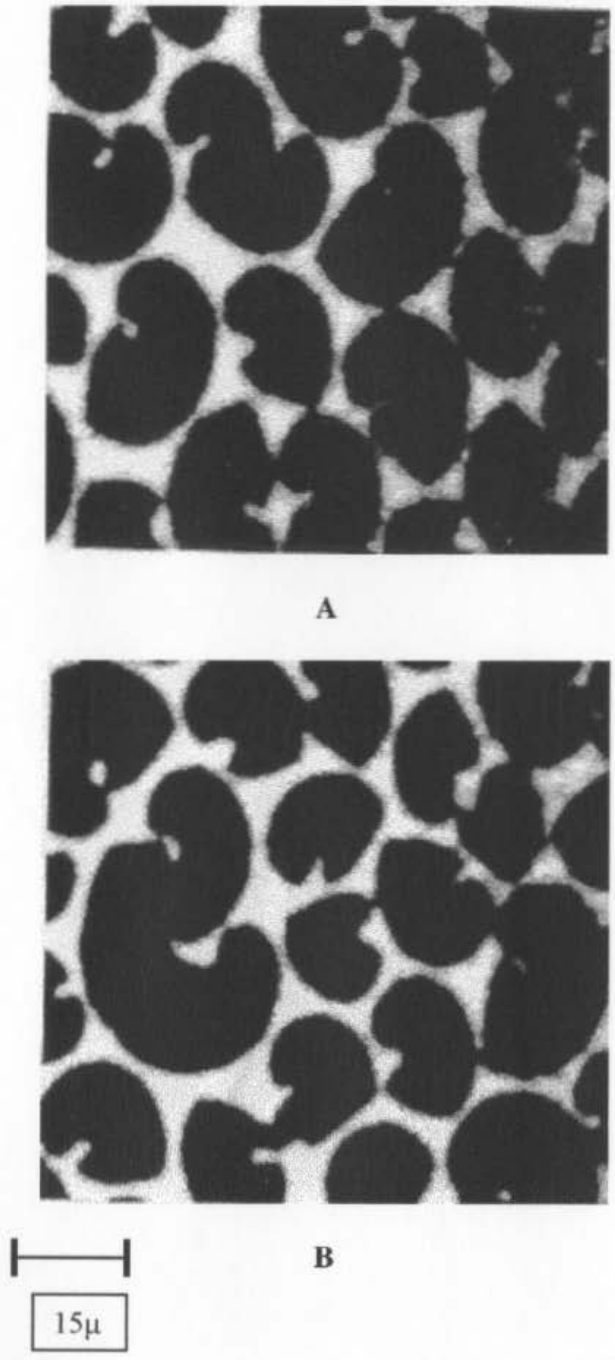

Fig. 4.23: DPPC domain shapes at 18 °C at π = 5.2 mN/m.

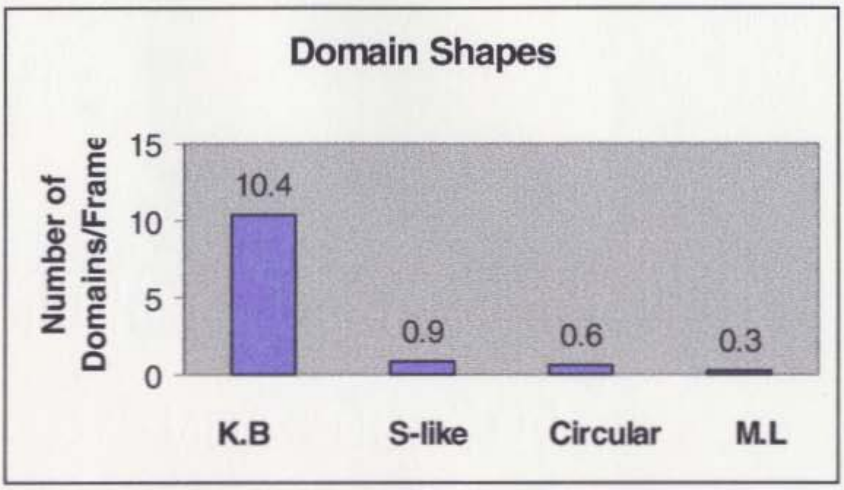

Fig. 4.24: DPPC domain shapes in the LE/LC coexistence region at surface pressure of 5.2 mN/m. at 18 °C.

4.7 Domain Visualization at Different Temperatures:

The study of pure DPPC domains yields valuable information that can help in understanding the behavior of the mixture of the DPPC with other materials such as PS.

Researchers are interested in visualizing the domains of DPPC at temperature of 37 °C utilizing fluorescence techniques. The evaporation of the subphase and its condensation at the lens of the objective of the microscopic system complicate the visualization of the domains at higher temperatures. To examine the merit of the modifications that have been introduced to the existing surface balance, visualizations at different temperatures have been reported in this study. The images have been captured and analyzed to determine the domain sizes at each temperature.

The condensation of the subphase on the objective lens have been minimized by introducing a Teflon sleeve that is surrounded by a heating coil as described previously in the experimental set-up chapter.

The following procedure was followed in order to get the images at different temperatures. For higher temperatures than the room temperature the heating procedure and its control were described previously.

The visualization of the domains was intended to be at the last point at the LE/LC coexistence region i.e. that just before the film starts to become totally liquid condensed. The visual observations have been carried out at surface pressure of: 5.3, 9, 14.5, 23, and 39 mN/m. for the isotherms of 18, 22, 26, 30, and 35 °C respectively. At each temperature, several visualizations have been performed in order to determine the point where LE/LC coexistence region ends. Once that point has been determined, the DPPC solution will be deposited to the subphase at a selected temperature. The 30 minutes

waiting time for the evaporation of the chloroform was applied. The compression was achieved at a slow rate -20 mm^2/molecule. The waiting time between compression steps was 2 minutes but at the point of visualization the wait was 15 minutes. It is worthwhile to note here that the protocol followed in higher temperature experiments is different from that followed in the experiment at 18 °C which was described in section 4.5. This waiting time was found to be convenient in order to let the domains grow enough so that good visualization can be achieved with the available microscope resolution. Of course at higher temperatures such as 35 °C the domains are very small.

At the point of visualization the cylindrical Teflon sleeve can be extended beyond the objective and touch the monolayer film at the surface of the subphase. Thus the Teflon sleeve has been manipulated to enclose a portion of the monolayer film at the surface. That can be achieved by lowering the sleeve a depth of one centimeter inside the subphase. The visualization has been performed with the enclosed surface area of 2.7 cm^2. The sleeve has been found to reduce the motion of the domains, especially at higher temperatures.

The observation of the domains usually started after 5 to 7 minutes from the time when the Teflon sleeve has been dipped into the subphase. This waiting time was introduced to ensure that the equilibrium between the enclosed domains and the rest of the monolayer is reached. After the 7 minutes waiting time the recording was performed.

Two experiments at room temperature were carried out in order to study the effect of the sleeve dipping on the size and shape of the domains. In one the "sleeve method" was utilized to visualize the domains while in the second has been performed without sleeve. No difference was found in the domain shape and size.

Visualizations at different temperatures-in the range from 18 °C to 35 °C -have been conducted exploiting the "sleeve method". The quality of the images still needs to be improved since the condensation was not totally eliminated. Condensation was observed to prevent the visualization after 15 to 20 minutes from the beginning of the recording. The time in which the condensation was eliminated has been found to be sufficient for recording procedure.

4.7.1 Images of domains in the coexistence region at 18 °C:

Fig.4.25 illustrates the DPPC domains at 18 °C and surface pressure of 5.3 mN/m. The objective lens -which has been utilized to record the images- was 50X. In order to compare the domain sizes with those imaged by the 40X objective, a transformation factor has been used. The size of the domains at this temperature is determined. The frequency distributions of the domain sizes for twenty frames have been plotted. From the histogram in Fig. 4.26 one can observe that the peak of the distribution is centered on 160 μ^2.

4.7.2. Images of domains in the coexistence region at 22 °C:

Fig. 4.27 illustrates the DPPC domains at 22 °C and surface pressure of 9 mN/m. The objective lens -which has been utilized to record images- was 50X. The sizes of the domains at this temperature are determined. The frequency distributions of the domain sizes for twenty frames have been plotted. From the histogram in Fig. 4.28 one can observe that the peak of the distribution is centered on 120 μ^2. Utilizing the same technique Nag has found the domain size at room temperature to be 1000 μ^2. His protocol in running the experiment is different from the experiment presented in this study. He waited for 10 minutes at each compression step. Moreover he has dissolved his DPPC in

a mixture of chloroform/methanol and he used deionized double distilled water with buffer [80].

4.7.3. Images of domains in the coexistence region at 26 °C:

Fig.4.29 illustrates the DPPC domains at 26 °C and surface pressure of 14.5 mN/m. The objective lens was 40X. The sizes of the domains at this temperature determined. The image quality needs to be enhanced. When eyepiece was used to visualize the domains at this temperature, small kidney beans were prominent. The domains appear as if they are not regular in shape. One possible reason for that may be the limitation in the resolution of the system.

The frequency distributions of the domain sizes for twenty frames have been plotted. From the histogram in Fig. 4.30 one can observe that the peak of the distribution is centered on 66 μ^2.

4.7.4. Images of domains in the coexistence region at 30 °C:

Fig.4.31 illustrates the DPPC domains at 30 °C and surface pressure of 23 mN/m. The objective lens was 40X. The domains seem to be circular. The sizes of the domains at this temperature were determined. The frequency distributions of the domain sizes for twenty frames have been plotted. From the histogram in Fig. 4.32 one can observe that the peak of the distribution is centered on 30 μ^2.

4.7.5. Images of domains in the coexistence region at 35 °C:

Fig.4.33 illustrates the DPPC domains at 35 °C and surface pressure of 39 mN/m. The objective lens was 40X. The sizes of the domains at this temperature were determined. The frequency distributions of the domain sizes for seventeen frames have been plotted. From the histogram in Fig. 4.34 one can observe that the peak of the distribution is centered on 9 μ^2.

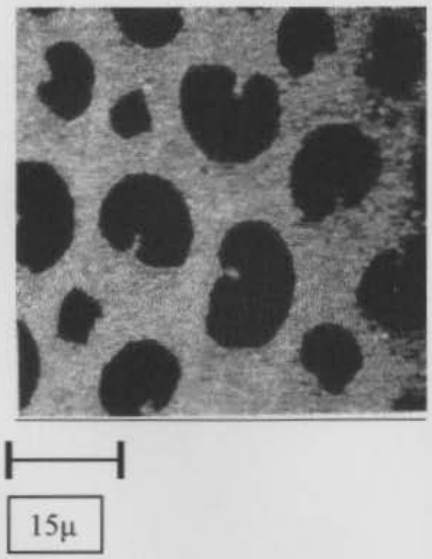

Fig. 4.25: The domain size at the last point of LE/LC coexistence region of DPPC film at 18 °C.

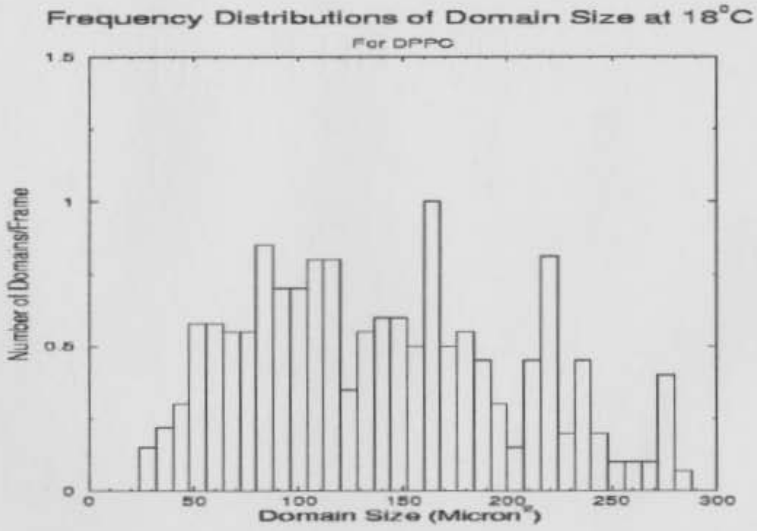

Fig. 4.26: Frequency distributions of domain *versus* their sizes at 18 °C.

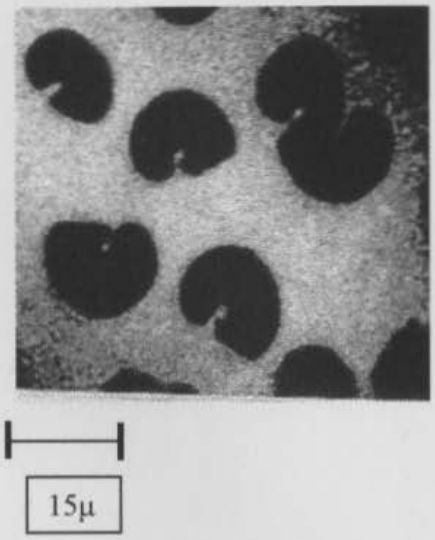

Fig. 4.27: The domain size at the last point of LE/LC coexistence region of DPPC film at 22 °C.

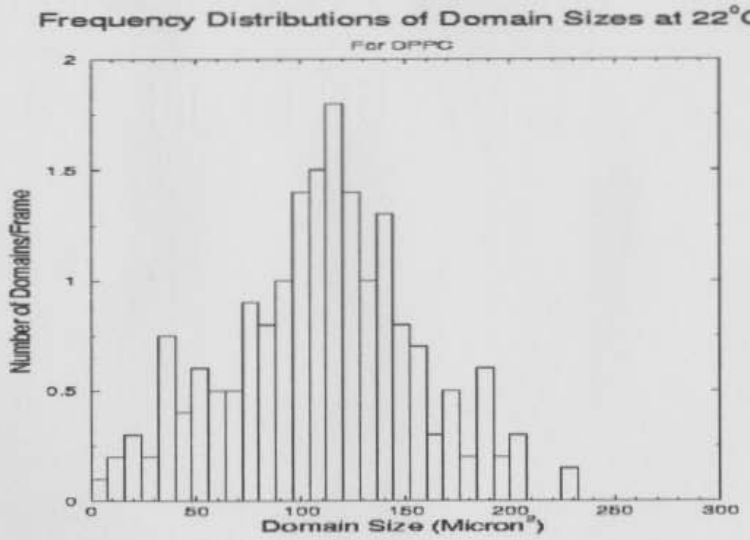

Fig. 4.28: Frequency distributions of domain *versus* their sizes at 22 °C.

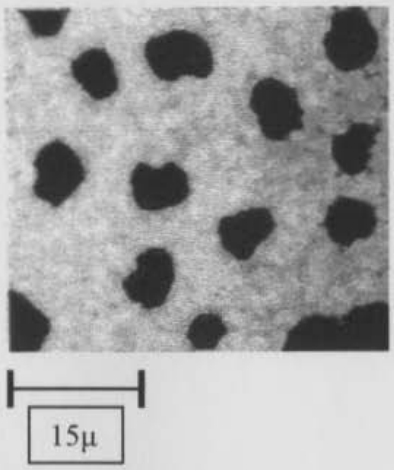

Fig. 4.29: The domain size at the last point of LE/LC coexistence region of DPPC film at 26 °C.

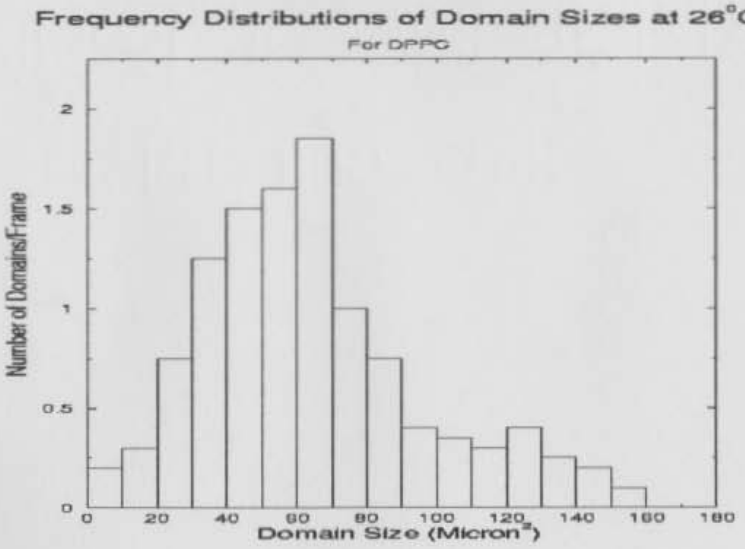

Fig.4.30: Frequency distributions of domain *versus* their sizes at 26 °C.

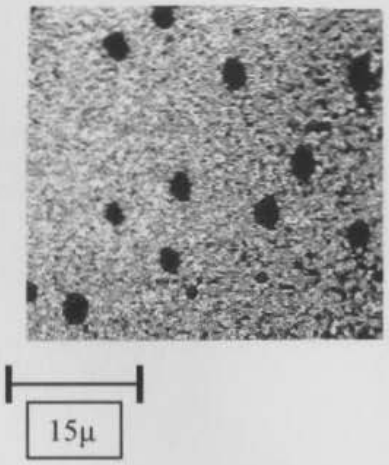

Fig. 4.31: The domain size at the last point of LE/LC coexistence region of DPPC film at 30 °C.

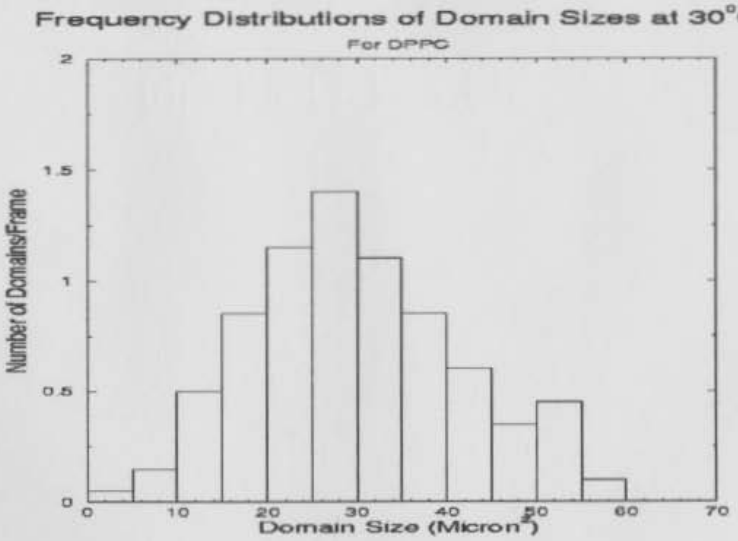

Fig. 4.32: Frequency distributions of domain *versus* their sizes at 30 °C.

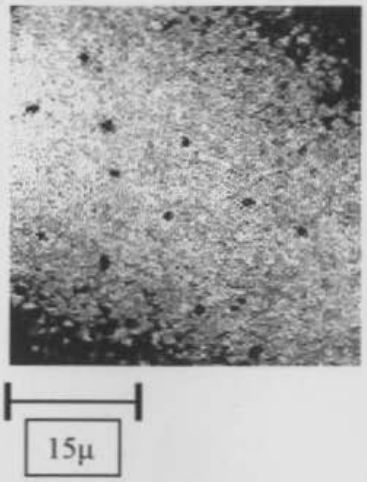

Fig. 4.33: The domain size at the last point of LE/LC coexistence region of DPPC film at 35 °C.

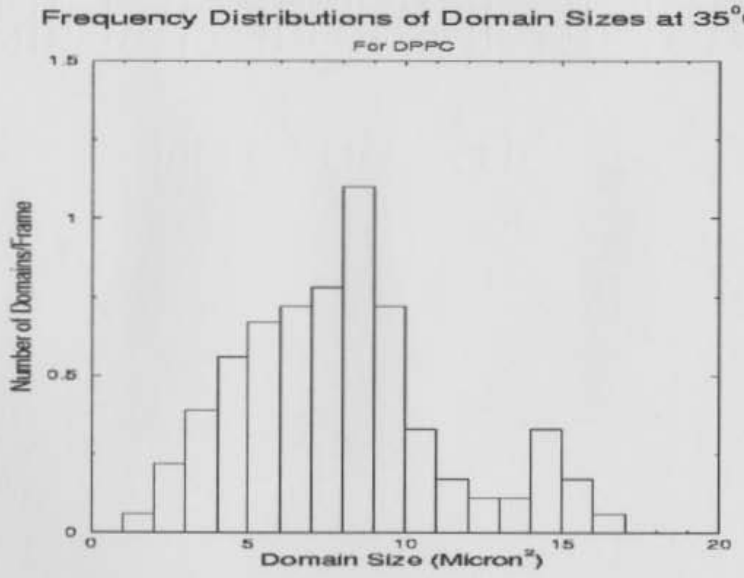

Fig. 4.34: Frequency distributions of domain *versus* their sizes at 35 °C.

4.8 DPPC Domain Size as Function of Temperature:

A relation between DPPC domain size at the last point of the LE/LC coexistence region and the temperature of the isotherm has been plotted in Fig.4.35. When the data are fitted quadratically one can observe that the domains are still there up to temperature around 38 °C. In the case of the linear fitting the domain size is observed to be zero at around 34.5 °C , which contradicts the theoretical expectation that the domain size should be finite up to the phase transition temperature of the DPPC which is 42 °C. The linear fitting might be misleading because of the small domain size at higher temperatures.

4.9 The Fraction in the Liquid Condensed phase as Function of Temperature:

Fig. 4.36 illustrates the fraction in the liquid condensed phase of DPPC as function of temperature of the film. On approaching the critical DPPC temperature the fraction of LC is getting smaller. The quadratic fitting can be valuable here since it can display some portion of the LC phase up to 35 °C while the linear fitting displays zero portion at 33.5 °C, which may not be the case.

From sections 4.8 and 4.9 one can realize that as temperature increases the monomolecular molecules film gain thermal energy that drives them from LC phase to LE phase.

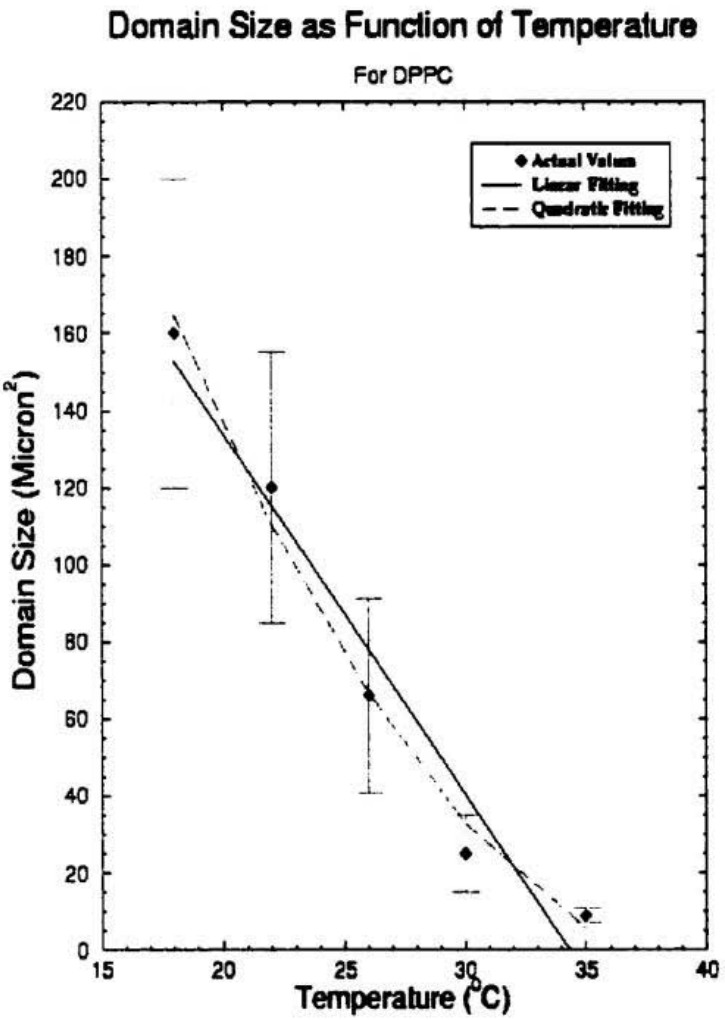

Fig. 4.35: The DPPC domain size as function of temperature. The lines are fitting lines.

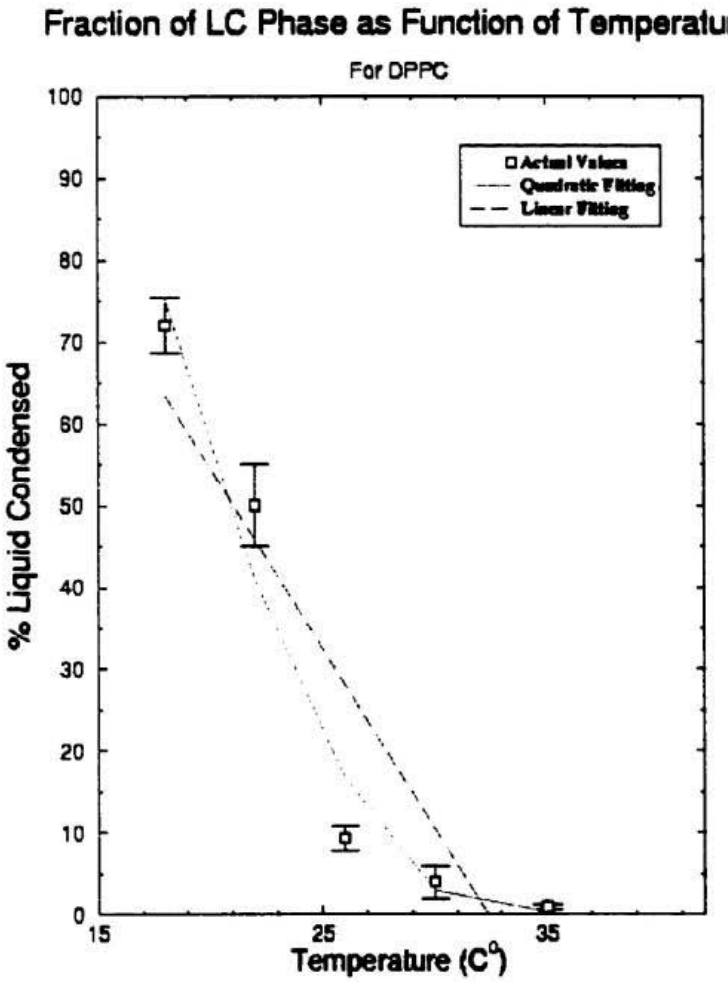

Fig. 4.36: The fraction of the liquid condensed phase of DPPC film as function of temperature. The lines are fitting lines.

CHAPTER FIVE

CONCLUSIONS

5. Conclusions

The study presented here is devoted to enhancing the existing epifluorescence surface balance (EFSB) so it can be utilized at different temperatures. In order to achieve that some modifications on temperature controlling and measuring systems have been introduced. Those have enabled us to work at higher temperatures up to 42 °C. Temperature could be controlled - after the modifications - within 0.5 °C.

A thermal insulating box with temperature control was introduced to isolate the force transducer. A teflon sleeve with heating coil was utilized to heat the objective lens. In order to improve temperature uniformity inside the enclosure, two fans were introduced. Four pots filled with the subphase material were located inside the enclosure to minimize the evaporation of the subphase. The entire enclosure was thermally isolated using an aluminum foil in order to minimize the temperature losses. To achieve precise temperature measurements, a set of thermocouples was introduced to the set-up. Those modifications have enabled us to obtain experimental results at higher temperatures.

π-A isotherms of two of phospholipids have been the subject of this study. The importance of DPPC in lung surfactant was the driving force to study its characteristics at different temperatures. We report the isotherms of DPPC at different temperatures - from 14 °C up to 42 °C. The agreement with the published data was good. Besides DPPC we measured DMPC isotherms in the temperature range from 6 °C to 23.3 °C. The agreement between the results reported here and the published data also is found to be good.

From the isotherms of both materials the latent heat of LE/LC phase transition has been calculated. The uncertainties involved in determining the area per molecule from the isotherms to some extent have influenced our results for the latent heat.

Both DPPC and DMPC have been studied by epifluorescence microscopy. Unfortunately, because of the resolution limitation for our monitoring system, we could not photograph the DMPC domains. The attached eyepiece has been utilized to visualize the domains by eye. They are very small and circular at 5 °C and surface pressure of 13 mN/m.

The domain sizes of DPPC at different temperatures and the fraction of the liquid condensed phase have been determined. We have observed as temperature increases - approaching melting chain temperature of DPPC- the average domain size decreases, as also does the fraction of liquid condensed.

Some uncertainties might have contributed to our results of the domain sizes. Those uncertainties are due to the method of determination of the area of the dark domains by surrounding them by a line. Sometimes the image is not so clear, especially at higher temperatures when the domain sizes are very small and moving very fast. In this case domains sizes are less accurately determined; the capture of their images in the monitor is not clear enough to enable exact determination of their areas.

Visualization of DPPC domains at higher temperatures than room temperature was a challenge to researchers. There are not many published observations of domain images at higher temperatures when EFSB is utilized. In this study we report a technique that has enabled us to carry out visual observation at higher temperature. We have eliminated the two major problems that were obstacles to working at higher temperatures.

Subphase condensation on the objective lens of the microscope prevents domain visualization. In this study we have developed a technique which has eliminated the problem. DPPC domains at different temperatures - up to 35 °C- have been visualized

utilizing this technique and quantitative analysis has been performed on the domain sizes. In order to examine the effect of the Teflon sleeve on domain shapes and sizes two experiments were conducted at room temperature, one with sleeve while the other without. We have concluded no difference has been observed in the sizes and shapes of the domains in both experiments.

The second problem was the thermal effect on our surface tension measuring system. By introducing heat isolating and heat controlling systems we have eliminated misleading results for the surface pressure.

The anticipated contribution of the study presented in this thesis will be to visualize the domains of Pulmonary Surfactant (PS) and others monolayer domains at higher temperatures. The study of pure DPPC domains at higher temperatures such as 37 °C can help in elucidating the behavior of mixtures of DPPC and other phospholipids in future. That can help researchers to get better understanding for the behavior of the components of those materials. Better understanding for the role of the PS at higher temperatures eventually will lead medical researchers to find a substitute for RDS and ARDS patients.

Bibliography

[1] M. C. Petty, *Langmuir-Blodgett Films. An Introduction* (Cambridge University Press, U.K, 1996).

[2] K. J. Klopfer and T. K. Vanderlick, J. Coll. Inte. Sci. **182**, 220 (1996).

[3] C. A. Helm and H. Möhwald, J. Phys. Chem. **92**, 1262 (1988).

[4] D. K. Rice, D. A. Cadenhead, R. N. A. Lewis, and R. N. McElhaney, Biochem. **26**, 3205 (1987).

[5] W. Hui, M. Cowdson, D. Papahadjopoulos, and D. F. Parsons, Biochim. Biophys Acta **382**, 265 (1975).

[6] J. Goerke and J. Gonzales, J. Appl. Physiol. **51**, 1108 (1981).

[7] K. Nag, C. Boland, N. Rich, K. M. Keough, Rev. Sci. Instrum. **61**, 11 (1990).

[8] C. W. McConlogue and T. K. Vandelick, Langmuir **13**, 7158 (1997).

[9] C. W. McConlogue, D. Malamud, and T. K. Vandelick, Biochi. Biophy. Acta. **1372**, 124 (1998).

[10] G. L. Gaines, Jr., *Insoluble Monolayers at the Liquid-Gas Interfaces* (J. Weily & sons, New York, 1966).

[11] I. Langmuir, J. Am. Chem. Soc. **39**, 1848 (1917).

[12] C. V. Raman and L.A. Ramdas, Phil. Mag. **3**, 220 (1927).

[13] J. W. McBain, R. C. Bacon, and H. D. Bruce, J. Chem. Phys. **7**, 818 (1939).

[14] I. Langmuir, Colloid Symposium Monographs **3**, 48 (1925).

[15] A. J. Walton, *Three Phases of Matter* (Clarendon Press, Oxford, 1983).

[16] N. K. Adam, *The Physics and Chemistry of Surfaces* (Oxford Press, U.K, 1930).

[17] I. Langmuir, J. Am. Chem. Soc. **38**, 221 (1916).

[18] I. Langmuir and V. J. Schaefer, J. Am. Chem. Soc. **59**, 2400 (1937).

[19] K. K. Eklund, J. Vuorinen, J. Mikkola, J. Virtanen, and Paavo. K. J. Kinnunen. Biochem. **27**, 3433 (1988).

[20] R. M. Weiss and H. M. McConnell, Nature **310**, 47 (1984).

[21] H. W. Fox and W. A. Zisman, Rev. Sci. Instr. **19**, 274 (1984).

[22] A. H. Ellison and W. A. Zisman, J. Phys. Chem . 60, 416 (1956).

[23] J. A. Mann and R. S. Hansen, Rev. Sci. Instr. **34**, 702 (1963).

[24] A. J. Allan, J. Coll. Sci. **13**, 273 (1958).

[25] K. Nag, N. Rich, and K. M Keough, Thin Solid Films **244**, 841(1994).

[26] D. M. Small, *The Physical Chemistry of Lipids From Alkanes to Phospholipids* (Plenum Press, New York, 1986).

[27] R. J. King and J. A. Clements, *The Biochemical Basis of Pulmonary Function*, **2** (Mercer Dekker Inc, New York, 1976).

[28] S. B. Hawgood, J. Benson, and R. L. Hamilton, Biochem. **24**, 184 (1985).

[29] S. Schürch, J. Goerke, and J. A. Clements, Proc. Nat. Acad. Sci. **75**, 3417 (1978).

[30] S. Schürch, Prog. Resp. Res. **18**, 1 (1984).

[31] M. E. Avery and J. Mead, A.M.A.J. Dis. Childr. **97**, 517 (1959).

[32] J. N. Hildebran, J. Goerke, and J. A. Clements, J. Appl. Physiol. **47**, 604 (1979).

[33] G. Enhorning, Prog. Resp. Res. **25**, 209 (1990).

[34] D. G. Ashbaugh, D. Bigelow, T. L. Petty, and B. E. Levine, Lancet **2**, 319 (1967).

[35] M. Hallman, T. A. Merrit, C. G. Cochrane, and L. Gluck, Prog. Resp. Res. **18**, 193 (1984).

[36] B. Muller, H. Hasche, G. Hohorst, W. Berhard, and D. Wichert, Prog. Resp. Res. **25**, 209 (1990).

[37] A. D. Bangham, C. J. Morley and M. C. Phillips, Biochim. Biophys. Acta **573**, 552 (1979).

[38] K. M. W. Keough, Prog. Resp. Res. **18**, 257 (1984).

[39] K. Nag, J. Perez-Gil, A. Cruz, N. Rich, and K. Keough, Biophys. J. **71**, 1356 (1996).

[40] S. Schürch, H. Bachofen, and E. R. Weibel, Resp. Physio. **62**, 31 (1985).

[41] R. H. Notter, S. A. Tabak, and R. D. Mavis, J. Lip. Res., **21**, 10 (1980)

[42] O. Albrecht, H. Gruler, and E. Sackmann, J. Physique 39, 301 (1978).

[43] M. C. Phillips and D. Chapman, Biochim. Biophys Acta **163**, 310 (1968).

[44] K. Tajima, and N. L. Gershfeld, Biophys. J. **47**, 203 (1985).

[45] N. L. Gershfeld, Biophys. J. **47**, 203 (1985).

[46] L. Ginsberg and N. L. Gershfeld, Biophys. J. **47**, 211 (1985).

[47] S. Subramanian and H. M. McConnell, J. Phys. Chem. 91, 1715 (1987).

[48] S. Stallberg-Stenhagen and E. Stenhagen, Nature **156**, 239 (1945).

[49] L. W. Horn, N. L. Gershfeld, Biophys. J. **18**, 3011 (1977).

[50] N. L. Gershfeld, J. Colloi. Inter. Sci. **85**, 28 (1982).

[51] A. Georgallas and D. A. Pink, J. Colloi. Inter. Sci. **89**, 107 (1982).

[52] D. A. Pink, M. J. Zuckermann, B. C. Sanctuary, and M. Costas, J. Chem. Phys.**76**, 4206 (1982).

[53] S. Henön and J. Meunier, J. Rev. Sci. Instrum. **62**, 936 (1991).

[54] D. Hönig and D. Möbius, Thin Solid Films **211**, 64 (1992).

[55] J. B. Li, R. Miller, D. Vollhardt, and H. Möhwald, Thin Solid Films **327-329**, 84 (1998).

[56] M. M. Lipp, K.Y. Lee, A. Waring, and J. Zasadzinski, Biophysi. J. **72**, 2783 (1997).

[57] Y. Fang and J. Yang, Biochi. Biophy. Acta. **1324**, 309 (1997).

[58] R. D. Neuman, S. Fereshtehkhou, and R. Ovalle, J. Colloi. Intr. Sci. **101**, 309

[59] H. Reinhardt-Schlegel, Y. Kawamura, T. Furuno, and H. Sasabe, J. Colloi. Inter. Sci. **147**, 295 (1991).

[60] N. Denicourt, P. Tancrēde, and J. Teissiē, Biophy. Chem. **49**, 153 (1994).

[61] R. A. Dlutty, M. L. Mitchell, T. Pettenski, and J. Beers, Applied Spectroscopy **42** N7, 125(1988).

[62] K. Kjaer, J. Als-Nielsen, C. A. Helm, L. A. Laxhuber, and H. Möhwald, Phy. Rev. Lett. **58**, 2224 (1987).

[63] J. A. Nielsen, F. Christensen, and P. S. Pershan, Phys. Rev. Lett. **48**, 1107 (1982).

[64] A. Breslau, M. Deutsch, and P. S. Pershan, and J. Bohr, Phys. Rev. Lett. **54**, 114 (1985).

[65] G. A. Overbeck and D. Mobius, J. Phys. Chem. **97**, 7999 (1993).

[66] G. Cevc, *Phospholipids Handbook* (Marcel Dekker Inc, New York, 1993).

[67] A. Miller and H. Möhwald, J. Chem. Phys. **86**, 4258 (1987).

[68] R. M. Weiss and H. M. McConnell, Nature **310**, 5972 (1984).

[69] M. Lösche, E. Sackmann, and H. Möhwald, Ber-Bunsenges. Phy. Chem. **87**, 848 (1983).

[70] B. Moore, C. M. Knobler, D. Broseta, and F. Rondelez, J. Chem. Soc. Farad. II. **82**, 1753 (1986).

[71] A. Miller and H. Möhwald, Europhys. Lett. **2**, 67 (1986).

[72] V. Von Tscharner and H. M. McConnell, Biophy. J. **36**, 409 (1981).

[73] M. Lösche, and H. Möhwald, Rev. Sci. Instrum. **55**, 1969 (1984).

[74] H. M. McConnell, L. K. Tamm, and R. M. Weiss, Proc. Nat. Acad. Sci. USA **81**, 3249 (1984).

[75] M. Lösche, H. P. Duwe, and H. Möhwald, J. of Collo. Interf. Sci. **126**, 432 (1988).

[76] S. Henön and J. Meunier, J. Chem. Phys. **98**, 9148 (1993).

[77] G. A. Overbeck and D. Honig, L. Wolthaus, M. Gnabe, and D. Mobius, Thin Solid Films **242**, 26 (1994).

[78] A. Fischer and E. Sackmann, J. Physiq. **45**, 517 (1984).

[79] B. G. Moore, C. M. Knobler, S. Akamatsu, and F. Rondelez, J. Phys. Chem. 94, 4588 (1990).

[80] K. Nag, C. Boland, N. Rich, and Kevin M. Keough, Biochi. Biophy. Acta. **1068**, 157 (1991).

[81] M. Flörsheimer and H. Möhwald, Chem. Phys. Lipids **49**, 231 (1989).

[82] T. Mavromoustakos and A. Papadopoulos, Life Sciences **62**, 1901 (1998).

[83] K. S. Birdi, *Lipid and Biopolymer Monolayers at Liquid Interfaces* (Plenum Press, New York, 1989).

[84] M. Blank, J. Phys. Chem. **66**, 1911 (1962).

[85] J. Cascales, Biophys. Chem. **69**, 1 (1997).

[86] A. Vonnahmen, A. Post, H. Galla, M. R. Sieber, Euro. Biophys. J. **26**, 359 (1997).

[87] D. J. Crisp, J. Colli. Sci. **11**, 356 (1956).

[88] N. K. Adam, J. Phys. Chem. **29**, 610 (1925).

[89] E. K. Rideal, J. Phys. Chem. **29**, 1585 (1925).

[90] K. B. Blodgett, Phys. Rev. **55**, 391 (1939).

[91] Personal Communications and Discussions with Co-workers.

[92] V. M. Kaganer, H. Möhwald, and P. Dutta, Rev. Mod. Phys. **71**, No.3, 779(1999).

Soc. **26**, 3205 (1987).